PHYSICOCHEMICAL PROPERTIES OF BEEF TONGUE AS A MEAT PRODUCT

by

SARAH EVANGELINE WARREN

(Under the Direction of Anand Mohan)

ABSTRACT

Demand for biological sources of protein is rising due to global population growth, rising incomes, and increased urbanization. Increasing the consumption of variety meats, including organs such as beef tongue, is one possible solution which would provide consumers with affordable meat products, generate revenue for the meat industry, and reduce food waste. Despite its potential as a nutritional and affordable meat product, little research has been done to characterize the physicochemical composition of beef tongue. In this study, the physicochemical composition of beef tongue was evaluated and characterized by determining proximate composition, proteomic profile, lipid composition, and histological profile (muscle structure, fiber size, and fiber type). The results show that beef tongue has the potential to be developed into a high-quality product for improving protein, fat, and nutrient content while greatly improving its value to the meat industry. Future research on beef tongue should focus on evaluating possible food applications.

INDEX WORDS: beef variety meats, beef tongue, protein, fatty acids, fiber type

PHYSICOCHEMICAL PROPERTIES OF BEEF TONGUE AS A MEAT PRODUCT

by

SARAH EVANGELINE WARREN

B.S., University of Georgia, 2014

A.B., University of Georgia, 2014

A Thesis Submitted to the Graduate Faculty of The University of Georgia in Partial Fulfillment of the Requirements for the Degree

MASTER OF SCIENCE

ATHENS, GEORGIA

2019

PHYSICOCHEMICAL PROPERTIES OF BEEF TONGUE AS A MEAT PRODUCT

by

SARAH EVANGELINE WARREN

Major Professor:	Anand Mohan
Committee:	Brian Bowker
	Rakesh K. Singh
	Kevin E. Mis Solval

Electronic Version Approved:

Ron Walcott
Interim Dean of the Graduate School
The University of Georgia
December 2019

DEDICATION

I would like to dedicate my thesis to my mother. From summer school with Ms. Rumpelstiltskin to experiments in the kitchen at home, you have instilled in me a love for science and taught me to never stop being curious. Thank you for all you have done for me.

ACKNOWLEDGEMENTS

First of all, I must thank Dr. Anand Mohan for advising me throughout my graduate studies and research. My project would also not have been possible without the overwhelming amount of guidance and assistance by Dr. Brian Bowker. I am very grateful as well to Dr. Rakesh Singh and Dr. Kevin Mis Solval for serving on my committee.

I would like to acknowledge Dr. Ronald Pegg, Dr. Chau-wen Chou, and David Parks for their help in the analysis of my samples. I would also like to thank Hannah LeClair for being the best office buddy I could ask for and Candace McKinney for all of her help in the lab.

Finally, I would like to thank my family and friends. Thank you especially to Dad, Emilie, Andrew, Pete, Frank, and Mehdi for all of your love and encouragement.

TABLE OF CONTENTS

Page

LIST OF TABLES

Page

LIST OF FIGURES

Page

CHAPTER 1

INTRODUCTION

Animal meat has been a large part of the traditional human diet and is known to provide both macro and micronutrients, including protein, fat, iron, selenium, folic acid, zinc, and vitamins A and B_{12} (Biesalski, 2005). Demand for animal-derived biological sources of protein is rising globally due to steady growth in human population, rising incomes, and increased urbanization. Trends toward high-protein diets further fuel protein demand (Boland et al., 2013). The Food and Agriculture Organization of the United Nations (FAO) has projected that global meat production must increase by an additional 200 million tons by 2050 in order to meet current predictions of food demand ("How to Feed the World in 2050," 2009). Variety meats, including organs such as heart, liver, kidney, and tongue, are likely to become more valuable food sources, and the meat industry must look for ways to market these products. With all of the nutritional advantages of animal food products, variety meats present a great economic opportunity for the meat industry. The efficient utilization of animal meat by-products is one possible solution which will reduce food waste in meat processing, generate revenues, and provide consumers with affordable food products.

Animal by-products, both edible and inedible, comprise a large portion of the meat industry's production. However, these products are often undervalued and underused. Total by-products are estimated to constitute about 44% of the live weight of cattle, while edible by-products are estimated to contribute 12%. Edible organs such as tongue, heart, liver, and kidney are categorized as variety meats and are usually sold or exported as is, with minimal processing.

Approximately one-fourth of the volume of beef exports from the United States is made up of edible by-products, indicating the significant value that these products add to the meat industry (Marti, Johnson, & Mathews, 2011). In 2016, the U.S. exported almost 280,000 metric tons of beef variety meat, which was valued at more than $754 million (Schaefer & Arp, 2017).

Currently, variety meats generate most of their economic value from the export market (Schaefer & Arp, 2017). For example, beef tongue is primarily exported to Northern Asia and Mexico. More than 90% of U.S. beef tongues are exported to these regions ("Market access triggers swings in beef variety meat values," 2013). In 2016, Japan imported 19,000 metric tons of beef tongue, valued at more than $286 million, illustrating the significant revenue that this variety meat generates for the meat industry (Schaefer & Arp, 2017). In Mexico, beef tongue is commonly used in tacos and soups, and in Japan it is often prepared as a grilled meat. In other parts of the world, beef tongue is consumed as a low-cost, high-quality source of protein and nutritional elements. Increasing the domestic consumption of beef tongue would add great value to the meat industry as well as provide an affordable nutritional product to consumers. In addition to the economic incentives, it is advantageous to salvage this animal waste as a valuable resource or convert it into a value-added ingredient.

Variety meats provide important nutrients such as protein, fatty acids, essential vitamins, and minerals. Beef tongue is a source of iron, zinc, choline, and vitamin B_{12}, as well as an excellent source of biologically available protein. Alao, Falowo, Chulayo, and Muchenje (2017) cited that each serving of beef tongue can provide about 28% of the recommended daily iron intake for men and 12% of the recommended intake for women. According to the USDA Food Composition Database (available online at https://ndb.nal.usda.gov/ndb/), a 3.5 ounce serving of beef tongue provides 14.78 g of protein, including all of the essential amino acids. Each serving

also provides 2.93 mg of iron, 2.85 mg of zinc, and 3.76 mg of vitamin B_{12}. Further, more than half of beef tongue's fatty acids are unsaturated ("Full Report (All Nutrients) 13339, Beef, variety meats and by-products, tongue, raw," 2018).

The meat industry has been using variety meats as nutritional and affordable meat products for a long time. Increasingly high nutritional standards and the rising cost of meat products warrant the innovative use of meat by-products. This research is a positive step in that direction by providing consumers and the meat industry with information on the nutritional and physicochemical composition of beef tongue. The knowledge generated from this research will allow for further utilization of beef tongue as a raw material for meat products. In light of the current research, beef tongue has the potential to be developed into a meat product with high-quality protein, fat, and nutrient content, thereby greatly improving its value to the meat industry. Currently, little research has been performed to analyze the biological and physicochemical composition of beef tongue. Therefore, this research study was undertaken to evaluate and characterize the physicochemical properties of beef tongue as a meat product. Specifically, objectives were to 1). determine the proximate composition, proteomic profile, and lipid profile of beef tongue; and 2). evaluate the fiber type, connective tissue, and histological composition (muscle structure, fiber size, and fiber type) of beef tongue. These parameters are expected to vary considerably in different regions of the tongue. Determining the extent of variation between regions will allow the meat industry to use beef tongue for a range of applications.

CHAPTER 2

LITERATURE REVIEW

2.1. Animal by-products

2.1.1. Economic value

Due to decreases in domestic consumption of variety meats and increases in global trade over the past century, variety meats now generate a majority of their economic value from the export market. The U.S. Meat Export Federation estimated that variety meat exports added $37.29 per head of cattle in 2016 (Schaefer & Arp, 2017). Some animal organs and meat by-products have very little demand in the domestic market and are almost entirely exported. For example, more than 90% of U.S. beef livers are exported to the Middle East, South America, and Russia. More than 75% of U.S. beef stomachs are exported to Mexico and Southeast Asia. Changes in these export markets can greatly impact revenue recovery for the U.S. meat industry. This impact was demonstrated in 2013 when Japan eased restrictions to allow the access of beef from U.S. cattle less than 30 months of age. The demand for beef tongues rose, and the price increased from $2 to $4 per pound. This price change was estimated to raise the value per head by $5.60 ("Market access triggers swings in beef variety meat values," 2013). Expanding the markets for variety meats is therefore in the meat industry's economic interest.

2.1.2. Nutrient content

Animal by-products, both edible and inedible, have a multitude of applications ranging from human food products and animal feed, to medical supplies and cosmetics. Variety meats, including organs such as heart, kidney, intestines, and liver, as well as by-products such as blood

and fat, contain many valuable nutrients. These include biological sources of high-quality proteins, fatty acids, essential vitamins, and minerals. Variety meats are rich in protein, and the essential amino acid content is similar to that of skeletal muscle (Nollet & Toldrá, 2011). In addition, organ meats typically have higher vitamin content than lean meats. Kidney and liver, for example, have been shown to contain between five and ten times more riboflavin than lean meat and are excellent sources of iron, folacin, and vitamins B_6 and B_{12}. Liver is also a good source of manganese, niacin, ascorbic acid, and vitamin A (Jayathilakan, Sultana, Radhakrishna, & Bawa, 2012).

2.1.3. Protein content

The high protein content of many animal by-products and variety meats contributes substantially to their nutritional value. Blood is a protein-rich by-product that has a wide variety of uses in the food industry, both functional and nutritive. It has long been used as an ingredient in Europe and Asia in products such as blood sausage, puddings, and soups. In food products, blood can be applied as a functional ingredient for emulsification, gelation, and foaming (Toldrá, Aristoy, Mora, & Reig, 2012). Collagen and gelatin, which is produced from the hydrolysis of collagen, are functional proteins that can be derived from animal by-products such as ears, feet, and skin. These proteins can be used as emulsifiers or fillers in meat products, stabilizers in desserts, or as sausage casings. They are also used in cosmetic products and by the pharmaceutical industry as capsule coverings (Jayathilakan et al., 2012).

2.1.4. Fat content

Animal by-products are also valuable sources of fat. Many organs, such as brain, heart, kidney, and liver, have higher levels of healthy polyunsaturated fatty acids (PUFAs) than lean meats (Jayathilakan et al., 2012). Ruminant animals, including cattle, have higher proportions of

PUFAs and lower proportions of saturated fatty acids (SFAs) than other species, including pork (Nollet & Toldrá, 2011). Meat fats have a long history of use in cooking and are valued for their functional properties and flavor attributes. Lard and tallow are meat fats traditionally used for deep fat frying or as shortening for pie crusts and cakes (Kincs, 1985). Rendered fat is also used in cosmetic products such as lotions and creams; more recently, animal fat has been used for biodiesel production as an environmentally-friendly alternative to traditional diesel fuel (Toldrá et al., 2012).

2.1.5. Other uses

Because the demand for variety meats is not as high as that for more valued meat cuts, and because some by-products are deemed unfit for human consumption, animal by-products have many applications outside of the food industry. These applications generate further revenue for the meat industry and reduce waste. In addition to the non-food applications mentioned above, animal by-products are frequently used as ingredients in pet food and animal feed. The pet food and animal feed industries value these by-products due to their high nutritional content and better digestibility than vegetable-based ingredients. Pet food and animal feed may also contain meat by-products that are deemed inedible for humans, such as bones, which provide a large supply of minerals (Corbin, 1992). Hides and skin contribute significantly to the total live-weight of animals and can therefore also generate large economic profit for the meat industry. Hides have been estimated to make up 59% of the by-product value of animals. A majority of this value comes from the production of leather (Ockerman & Hansen, 2000). Other uses for by-products considered inedible for humans include soap from rendered fat and glue from gelatin (Nollet & Toldrá, 2011).

Intestines have a multitude of applications as both food and non-food products. One of the most economically valuable uses of intestine is as sausage casings. Outside of the food industry, they are manufactured into musical instrument and tennis racket strings, surgical sutures, and fertilizers (Ockerman & Hansen, 2000).

The meat industry can generate a large amount of revenue from efficient utilization of animal by-products. The applications discussed above indicate the wide variety of functions these by-products can serve. The exploration of further uses will serve to increase their value to the meat industry and supply useful products for consumers.

2.2. Beef tongue

Beef tongue is a variety meat that has the potential to be applied in the meat industry as a source of high-quality protein and other nutritional elements. However, limited research has been conducted to evaluate beef tongue's physicochemical composition and potential applications as a meat product. There are a few studies that have focused on microbiological, sensory, and quality attributes of beef tongue. One study published in 1985 examined the effect of various chilling/freezing treatments on the microbiological quality of tongues (Vanderzant et al., 1985). Visser, Koolmes, and Bijker (1988) analyzed the effect of lactic acid treatments on the keeping quality of veal calf tongues. Another study by Miller et al. (1988) evaluated the chemical and sensory properties of jerky prepared from beef tongue, top round, and heart. A more recent study demonstrated the effects of processing with liquid smoke on the microbiological, sensory, and chemical characteristics of smoked beef tongue (Gonulalan, Kose, & Yetim, 2004).

2.3. Muscle composition

Factors including fatty acid content, protein profile, and muscle structure all influence the quality and value of a meat product, so investigation into these characteristics of beef tongue will aid the meat industry in capitalizing on its untapped potential as a valuable meat product.

Fatty acids in meat products contribute to quality due to effects on texture, flavor, oxidative stability, and nutritional value. Specifically, meat is a source of essential fatty acids, including ω-6 linoleic acid and ω-3 α-linolenic acid. Further, increased fat content has been shown to influence tenderness and juiciness, particularly in burgers or patties (Wood et al., 2008). Despite recommendations to limit red meat intake due to its saturated fatty acid (SFA) content, beef is rich in healthy monounsaturated fatty acids (MUFAs) and is a source of polyunsaturated fatty acids (PUFAs), including long-chain ω-3s (Vahmani et al., 2015). Oleic acid, an essential fatty acid found in meat, is the most significant MUFA in the human diet and is valued for its health benefits, including the reduction of coronary heart disease risk (Lopez-Huertas, 2010). Siedler, Springer, Slover, and Kizlaitis (1964) determined the fatty acid composition of variety meats, including beef tongue. The study found that the oleic acid composition in tongue was 44% of the total fatty acid content. This was the highest of all beef variety meats tested (including kidney, liver, and heart). Despite the health benefits of PUFAs, their multiple unsaturated bonds make them more susceptible to oxidation than MUFAs, adversely affecting the shelf-life stability and quality of PUFA-rich meat products (Tao, 2015).

Meat plays a major role in the human diet as a source of protein. The protein composition of a muscle tissue influences the ultimate quality of a meat product due to effects on texture, color, flavor, and nutritional value (Listrat et al., 2016). The proteins found in muscle are classified as myofibrillar, sarcoplasmic, or connective (stromal). Myofibrillar proteins are the

structural proteins responsible for contraction of muscle fibers. Actin and myosin are the two major myofibrillar proteins involved in contraction. Sarcoplasmic proteins are found in the fluid cytoplasm (or sarcoplasm) of muscle cells and include many of the enzymes involved in muscle metabolism. Stromal proteins make up the connective tissue that provides structure and support for muscles (Pearson & Young, 1989). Proteomic analysis can give information on the exact composition and quantity of proteins in a muscle tissue.

Factors such as breed, diet, age, and sex can influence muscle composition in cattle. For example, fat deposition is reported to be a heritable trait and varies significantly among breeds. In terms of diet, grass-fed cattle tend to have lower overall fat content than grain-finished cattle. Skeletal muscle from grass-fed cattle tends to have higher percentages of PUFAs but lower percentages of MUFAs (Van Elswyk & McNeill, 2014). Cattle age and sex have been shown to influence the amount of intramuscular collagen cross-linking (Listrat et al., 2016). However, these factors affect individual muscles in different ways, and the extent of their influence on variety meats, including beef tongue, is currently unknown.

2.4. Muscle structure

Histological analysis can provide further insight on the structure and composition of a muscle tissue. Skeletal muscle is composed of approximately 90% muscle fibers and 10% connective and adipose tissue (fat). Muscle fiber size, connective tissue distribution, and lipid composition affect the color, texture, and flavor of meat. Muscle fibers range from 10 to 100 μm in diameter and can reach up to several centimeters in length. Muscle fibers contain multiple myofibrils, themselves made up of many repeating sarcomeres which are responsible for muscle contraction (Listrat et al., 2016).

Histological stains are used for highlighting and comparing various features of muscle tissue. The hematoxylin-eosin (H&E) stain is a routine stain that dyes nuclei, ribosomes, and rough endoplasmic reticulum blue due to their affinity for hematoxylin. The cytoplasm, most organelles, and the extracellular matrix are dyed pink due to their affinity for eosin (Chan, 2014). This stain allows for the visualization of cell structure and the organization of the tissue as a whole. The Oil Red O stain is used to differentiate neutral triglycerides. Lipids will appear as red drops, while nuclear components will be dyed blue (Christoffersen & Thomsen, 2014). The intramuscular fat content of a muscle sample can be visualized using this staining procedure. Muscle adipocytes, cells responsible for the storage of triglycerides, are found between fibers and fiber bundles (Listrat et al., 2016). Masson's trichrome stain is used to distinguish connective tissue, in particular collagen, by dyeing it bright blue (Martinello et al., 2015). In skeletal muscle, connective tissue is classified as endomysium, which surrounds individual muscle fibers, perimysium, which surrounds muscle fiber bundles, or epimysium, which surrounds entire muscles (Listrat et al., 2016).

The complicated relationships between meat product sensory qualities and histological muscle tissue features such as connective tissue, intramuscular fat, and fiber size have been explored. Intramuscular fat has been found to positively correlate with tenderness, juiciness, and flavor. Connective tissue also plays a role in determining meat tenderness, particularly in cooked meat. When heated, collagen is thermally denatured, or gelatinized. The impact on tenderness depends on the degree of cross-linking and the structure of the endomysium and perimysium (Listrat et al., 2016).

The sarcomere structure is also known to influence tenderness, with shorter sarcomere lengths associated with tougher cooked meat (Ertbjerg & Puolanne, 2017). Increasing sarcomere

length up to 2.0 μm has been correlated with increased tenderness (Wheeler, Shackelford, & Koohmaraie, 2000). Likewise, a study by Rhee, Wheeler, Shackelford, and Koohmaraie (2004) found that four of the five most tender muscles analyzed had sarcomere lengths greater than 2.0 μm. Various studies have demonstrated a negative correlation between fiber size, specifically cross-sectional area (CSA), and beef tenderness (Listrat et al., 2016; Joo, Kim, Hwang, & Ryu, 2013; Seideman, Koohmaraie, & Crouse, 1988). That is, muscles with lower CSA can be expected to produce more tender meat. Despite these studies' efforts to determine the relationships between muscle characteristics and meat quality, the complex interactions between these characteristics make the ultimate quality of a meat product difficult to predict. Other factors such as sex, age, and breed further complicate the relationships (Listrat et al., 2016).

2.5. Muscle fiber types

Another important biochemical characteristic of muscle is fiber type composition and the associated metabolic properties. Muscles employ two major metabolic pathways: the oxidative or aerobic pathway, which generates ATP through oxidative phosphorylation in the mitochondria, and the glycolytic or anaerobic pathway, which generates a smaller amount of ATP and converts pyruvate into lactic acid in the sarcoplasm. Muscles fibers that rely more on the oxidative pathway to generate energy contain greater concentrations of mitochondria and the enzymes required for oxidative metabolism. These include the enzymes involved in the TCA cycle, electron transport, oxidative phosphorylation, and β-oxidation, as well as pyruvate dehydrogenase (Voet, Voet, & Pratt, 2006).

Muscles are classified into metabolic fiber types based on their reliance on either the oxidative or glycolytic pathway (Listrat et al., 2016). The terms red and white fiber can be used as basic descriptors of fiber type. These names derive from the fibers' relative richness in the

oxygen-carrying protein myoglobin, which gives meat its red color. Red fibers have higher oxidative activity and contract slower than white fibers, which have greater glycolytic activity and contract faster. There are also intermediate fibers, which have both oxidative and glycolytic activity. Muscle fibers can also be classified as type I or II. Type I fibers are generally red fibers. Type II fibers are divided into type IIA or type IIB. Type IIA are fast-twitch intermediate fibers, with both oxidative and glycolytic activity. Type IIB are fast-twitch fibers that have a primarily glycolytic metabolism, similar to white fibers (Pearson & Young, 1989).

Muscle fiber type can impact the overall quality of a meat product. However, like the relationship of meat quality with other muscle characteristics, it is difficult to predict due to the interaction of many factors, including age and breed. A study on Hanwoo cattle in Korea found an increased percentage of type I (red) fibers to improve marbling and tenderness (Hwang, Kim, Jeong, Hur, & Joo, 2010). Similarly, researchers studying meat quality characteristics of indigenous African cattle breeds found muscles with a higher proportion of white fibers to be less tender (Strydom, Naude, Smith, Scholtz, & van Wyk, 2000). Fiber type also influences the juiciness and flavor of meat. A high proportion of type I (red) fibers has been associated with greater juiciness and improved flavor, likely due to a higher phospholipid content in these fibers (Listrat et al., 2016).

Fiber type has also been shown to have a correlation with fiber size. Slow-twitch, oxidative muscle fibers are generally smaller than fast-twitch, glycolytic fibers (van Wessel, de Haan, van der Laarse, & Jaspers, 2010). van der Laarse, des Tombe, Lee-de Groot, and Diegenbach (1998) also found that skeletal muscle fibers with greater maximum rates of oxygen consumption (i.e. more oxidative fibers) had lower CSA than those with lower maximum rates.

2.6. Human tongue

Although beef tongue has not been explicitly investigated, the human tongue has been studied. The intrinsic muscles comprising the main body of the human tongue have been shown to overlap and interweave extensively and are responsible for the tongue's wide range of movements and ability to change shape. Although they likely share many similar features, the human tongue is expected to be somewhat more complex than that of other species, due to the unique movements required for speech (Sanders & Mu, 2013). Sanders, Mu, Amirali, Su, and Sobotka (2013) performed fiber-typing of human tongue muscle and found 54% of fibers to be slow-twitch (type I). Stål, Marklund, Thornell, De Paul, and Eriksson (2003) found 60% of fibers to be type II, although there were significant regional differences. The posterior region had a higher proportion of type I fibers than the anterior region, where type II fibers predominated. They concluded that the composition differences were likely due to differences in function. The anterior region of the tongue requires quick movement, whereas the posterior region has relatively slower movements and maintains them for a longer time.

A physicochemical study of beef tongue muscle, involving the discussed characteristics, will provide valuable information to the meat industry regarding an underutilized meat product. The knowledge gained through this study will aid in improving the application of beef tongue as a high-quality meat product that can provide nutritional value to consumers and economic benefit to the meat industry.

CHAPTER 3

MATERIALS AND METHODS

3.1. Raw materials

Frozen beef tongues, *Longissimus dorsi* (IMPS# 1112A), and hearts from grass-fed cattle slaughtered at 30 months or earlier were obtained from a local beef purveyor. The tongues were shipped and stored frozen at -20 °C and thawed at 4 °C for 24 hours prior to analysis. All chemicals used were of analytical grade.

3.2. Proximate composition

Samples (15 g) were cut from the anterior, anteromedial, posteromedial, and posterior regions of a thawed, peeled beef tongue (see Figure 1 for a diagram of sampling regions). The tongue was first cut in half to mark the division between anteromedial and posteromedial. The posterior region was the thickest portion of the tongue, which formed the tongue's root or base in the cow's mouth. The anterior region was the thinnest portion of the tongue, starting from the apex. Visible connective tissue and fat were trimmed during sampling. Samples were analyzed for moisture by oven drying at 105 °C for 3 hours (AOAC Method 930.15). An ANKOM^{XT15} Extractor (PVM 1:2003 and AOCS Procedure Am 5-04) was used to analyze fat content. Protein was analyzed by the Kjeldahl method (AOAC Methods 4500-N_{org} C and 4500-NH_3 C) and total ash using a muffle furnace at 600 °C for 2 hours (AOAC Method 942.05). All experiments were replicated for a minimum of three times at different occasions.

3.3. Protein analyses

The sarcoplasmic and myofibrillar protein fractions were isolated from beef tongue, *Longissimus dorsi* (*L. dorsi*), and beef heart according to the protocols of Goll, Young, and Stromer (1974) and Doerscher, Briggs, and Lonergan (2004) with modification. Excess fat and connective tissue were trimmed before cutting into small pieces and mincing. A 1.5 g sample was weighed into a 50 mL round bottom centrifuge tube. Homogenization buffer (15 mL; 100 mM Tris, 10 mM EDTA, pH 8.3) was added to the tube, and the sample was homogenized with a homogenizer (VWR 250; 5,000 rpm, 3 x 10 sec). The samples were centrifuged at 1,000 *g* for 20 minutes at 4 °C. The supernatant was removed and further clarified by centrifugation at 48,000 *g* for 30 minutes at 4 °C. The resulting supernatant, containing the sarcoplasmic protein fraction, was filtered through cheesecloth and stored at 4 °C for protein concentration determination. The pellet was discarded.

To isolate the myofibrillar fraction, the pellet from the first centrifugation step was resuspended in 10 mL of a standard salt solution (100 mM KCl, 20 mM K_2HPO_4/KH_2PO_4, pH 7.0, 2 mM $MgCl_2$, 1 mM EGTA, 1 mM NaN_3) and homogenized (5,000 rpm, 10 sec). The samples were centrifuged at 1,000 *g* for 10 minutes at 4 °C. This resuspension, homogenization, and centrifugation procedure was repeated for at least three times.

After the third centrifugation step, the pellets were resuspended in 10 mL of the salt solution plus 1% Triton X-100 (Fisher Scientific, Pennsylvania, USA) and homogenized. The samples were subjected to two resuspension and centrifugation steps at 1,500 *g* for 10 minutes at 4 °C. The pellets were then resuspended in 10 mL of the standard salt solution, vortexed, and centrifuged at 1,500 *g* for 10 minutes at 4 °C. This step was performed twice, and the supernatant was discarded. The final pellet, containing the isolated myofibrillar protein fraction was weighed

and resuspended in four volumes of a resuspension buffer (100 mM KCl, 5 mM Tris, pH 7.0) and vortexed.

A biuret protein assay was performed to determine the protein concentration of both fractions (myofibrillar and sarcoplasmic) for each sample. For the standard curve, serial dilutions of bovine serum albumin (BSA) standards (Sigma-Aldrich, Missouri, USA) were added in triplicate to a 96-well microplate along with appropriate amounts of deionized water and biuret reagent (Sigma-Aldrich, Missouri, USA) to final BSA concentrations of 0, 1, 2, 3, 4, and 5 mg/mL and a final volume of 250 μL. For sarcoplasmic samples, 50 μL of sample, 75 μL of deionized water, and 125 μL of biuret reagent were added to 6 wells. For myofibrillar samples, 25 μL of sample, 100 μL of deionized water, and 125 μL of biuret reagent were added to 6 wells. The plates were incubated at room temperature for 20 minutes and the absorbance was recorded at 540 nm. After determining the protein concentration of each fraction, an aliquot of each (sarcoplasmic and myofibrillar fractions) was denatured for 3 minutes at 100 °C in a thiourea/urea sample buffer (8 M urea, 2 M thiourea, 3% SDS (w/v), 75 mM dithiothreitol, 25 mM Tris-HCl (pH 6.8), 0.004% bromophenol blue) to a final volume of 500 μL and a protein concentration of 2 mg/mL. These denatured fractions were stored at -20 °C.

The protein fractions were separated using sodium dodecyl sulfate polyacrylamide gel electrophoresis (SDS-PAGE). A 4-20% gradient Tris-Glycine gel (Thermo Fisher Scientific, Massachusetts, USA) was loaded with 5 μL of denatured sample per lane. The first lane of each gel was loaded with 3 μL of a broad range unstained protein ladder (PageRuler™, Thermo Scientific, Massachusetts, USA). The gels were run in running buffer (25 mM Tris (pH 8.3), 192 mM glycine, 2 mM EDTA, 0.1% SDS (w/v)) at 4 °C. The gels were run at 100 V for 10-30 minutes, or until the samples had entered the gel 2-3 cm. The voltage was increased to 150-200

V for a total run time of 1.5-2 hours. Gels were stained for 2 hours in 0.1% (w/v) Coomassie brilliant blue R-250, 40% methanol, and 7% acetic acid and destained in 40% methanol and 7% acetic acid.

3.4. Trypsin digestion and protein identification

Protein profiling was performed using liquid chromatography-mass spectrometry (LC-MS) analysis on the isolated sarcoplasmic fractions of beef tongue and *L. dorsi* (concentration determined to be 5 μg/μL by biuret protein assay). A 10 μg sample was thawed and diluted with 10 μL of 20 mM ammonium bicarbonate. The sample was denatured by a heat block at 100 °C for 5 minutes. The denatured proteins were reacted at room temperature with 2 μL of 10 mM dithioreitol in 20 mM ammonium bicarbonate for 20 minutes and alkylated with 2 μL of 0.1 M iodoacetamide for 20 minutes in the dark. A 0.2 μg aliquot of trypsin (0.01 μg/μL in 20 mM ammonium bicarbonate) was added for protein digestion overnight in a 37 °C oven. The sample was then dried in a vacufuge and resuspended in 20 μL of 2% acetonitrile/0.1% formic acid.

An LTQ Orbitrap Elite Mass Spectrometer coupled with a Proxeon Easy NanoLC system (Thermo Fisher Scientific, Massachusetts, USA), located at the Proteomics and Mass Spectrometry Facility, University of Georgia, was used for mass spectrometry analysis of the samples. A 1-2 μL aliquot of the peptides were loaded onto a reversed-phase column (self-packed column/emitter with 200 Å 5 μM Bruker MagicAQ C18 resin) and directly eluted into the mass spectrometer. A two-buffer gradient elution (buffer A: 0.1% formic acid, buffer B: 99.9% acetonitrile with 0.1% formic acid) held at 0% buffer B for 2 minutes, then increased to 40% buffer B in 95 minutes and 95% buffer B in 10 minutes.

MS data was acquired by the data-dependent acquisition (DDA) method. First, a survey MS scan was acquired. The top 5 ions in the MS scan were then selected for, following collision-

induced dissociation (CID) and higher energy collisional dissociation (HCD) tandem mass spectrometry (MS/MS) analysis. The MS and MS/MS scans were acquired at resolutions of 120,000 and 30,000, respectively.

Xcalibur software (version 2.2, Thermo Fisher Scientific, Massachusetts, USA) was used for peak detection. Thermo Proteome Discoverer (version 1.4) with Mascot (Matrix Science Massachusetts, USA) and the Uniprot database were used for protein identification and modification characterization. Accuracy was verified by inspecting the spectra of possible modified peptides. A label-free quantification workflow in Proteome Discoverer allowed for the semi-quantitative analyses. Abundance of each protein was determined by the peak area.

3.5. Fatty acid profile

Three frozen beef tongues were thawed at 4 °C, and a 30 g portion of muscle tissue was cut from the anterior, medial, and posterior regions (as shown in Figure 1). Samples were refrozen at -20 °C prior to analysis. Fatty acid composition was analyzed according to the protocol of Gong et al. (2017). Lipids were extracted from each sample by the slightly modified Bligh-Dyer method and derivatized to fatty acid methyl esters (FAMEs) before being analyzed by gas chromatography-flame ionization detection (GC-FID). Approximately 80 mg of the extracted lipids was added to a 5 mL Reacti-vial™ (Thermo Fisher Scientific, Massachusetts, USA), and the exact mass was recorded. An internal standard, heptadecanoic acid (300 μL of 20 mg/mL hexanes) was added, along with the transmethylation reagent (2 mL of 6% v/v H_2SO_4 in anhydrous CH_3OH containing ~20 mg hydroquinone) and a triangle-shaped stir bar. The vials were capped, vortexed for 30 seconds, and placed in a Reacti-Block™ B-1 aluminum block within a Reacti-Therm III™ Heating/Stirring Module (Thermo Fisher Scientific, Massachusetts, USA) at 65 °C for 18 hours for further derivatization. The vials were cooled to approximately 23

°C, and 1 mL of deionized water was added. The resulting FAMEs were extracted three times with 1.5 mL of hexanes, followed by washing two times with deionized water. An N-EVAP® nitrogen evaporator (Organomation Associates, Inc., Massachusetts, USA) was used to remove the hexanes under a nitrogen stream, before again dissolving the FAMEs in 5 mL of hexanes. A 750 μL aliquot of the dissolved FAMEs was transferred to a 2 mL wide-opening crimp-top vial (Agilent Technologies, California, USA), along with 1 mL of hexanes. A polytetrafluoroethylene (PTFE)/red rubber septum and an 11-mm silver aluminum cap were placed to cover the vial, and it was crimped with an electronic crimper (Agilent Technologies, California, USA).

For fatty acid analysis, an Agilent 6890N GC-FID system equipped with electronic pneumatic control (EPC) split/splitless injector and a 7683 autosampler module was used, with a Supelco SP-2560 highly polar biscyanopropyl column (0.25 mm x 100 mm, 0.20 μm film thickness). A split ratio of 50:1 was employed, with ultra-high purity (UHP) grade helium as the carrier gas and column head pressure at 60 psi. The fuel gases for the FID were UHP-grade hydrogen and scientific-grade air at 450 and 40 mL/min, respectively. The oven was set to initially hold at 140 ℃ for 5 minutes, followed by ramping up at a rate of 4 ℃/min to a final temperature of 240 ℃, which was held for 15 minutes.

The FAMEs were identified by retention time mapping against a FAME reference standard mixture (Code No.: GLC-463, Nu-Chek Prep., Inc., Minnesota, USA). A relative response factor was calculated for each FAME and used for quantification. The analyses of nine samples were performed in duplicate and averaged for statistical analyses.

3.6. Histological analyses

Three fresh, never frozen tongues were stored at 4 °C prior to analysis. Each tongue was cut into anterior, medial, and posterior regions (as shown in Figure 1). Each region was peeled

and dissected using sterile scalpels to prepare strips approximately 1 cm wide, 1 cm high, and 3-6 cm long, cutting parallel to the apparent muscle fibers. Strips were prepared from the surface and interior muscles of each tongue region. Each strip was tied to a popsicle stick, frozen in isopentane chilled with liquid nitrogen, and stored at -80 ℃.

Cross-sections (10-12 μm thick) were cut from the frozen tongue strips using a Leica CM3050 S cryostat held at -20 °C and mounted on glass slides for staining. Approximately 10 slides were prepared from each of the 18 sampling locations. These slides were used for staining, including fiber typing.

Hematoxylin and eosin (H&E), Masson's trichrome, and Oil Red O stains were applied to duplicate slides from each location. For H&E staining, duplicate slides were fixed in 10% neutral buffered formalin (25 mL formalin + 1 g NaH_2PO_4 + 1.625 g Na_2HPO_4 + 225 mL deionized water) for 5 minutes. After being washed in deionized water for 1 minute, the slides were soaked in premade Mayer's hematoxylin stain (Sigma-Aldrich, Missouri, USA) for 30 minutes. These were then rinsed with deionized water and soaked in a 0.5% eosin/0.025% acetic acid stain (1 g eosin + 200 mL 95% ethanol + 50 μL glacial acetic acid) for 30 minutes. The eosin stain was removed by washing in deionized water. The slides were then placed in 70% ethanol for 1 minute, followed by 90% ethanol for 30 seconds, 100% ethanol for 30 seconds, and two rounds of soaking in xylene for 30 seconds. Cytoseal™ 60 mounting media with a coverslip was used for sealing the slides.

For Masson's trichrome stain, duplicate slides were fixed in 10% neutral buffered formalin (37-40%) for 1 hour and refixed overnight in Bouin's solution (5 mL glacial acetic acid + 25 mL formaldehyde + 75 mL saturated picric acid) at ambient temperature. The slides were rinsed with deionized water before soaking for 7 minutes in Weigert's iron hematoxylin mix

(solution A: 5.0 g hematoxylin + 500 mL 95% ethyl alcohol, solution B: 5.8 g ferric chloride + 495 mL deionized water + 5 mL concentrated HCl). Deionized water was used for washing the slides before incubating for 5 minutes in Biebrich scarlet-acid fuchsin solution (2.7 g Biebrich scarlet + 0.3 g acid fuchsin + 300 mL deionized water + 3 mL glacial acetic acid). The slides were further soaked in deionized water and later incubated for 10 minutes in phosphotungstic/phosphomolybdic acid solution (6.25 g phosphomolybdic acid + 6.25 g phosphotungstic acid + 500 mL deionized water), until the collagen color changed from red to maroon. This step was followed by a 7-minute incubation in aniline blue solution (2.5 g aniline blue + 100 mL deionized water + 1 mL glacial acetic acid). The slides were soaked in deionized water, incubated in 1% glacial acetic acid for 1.5 minutes, and again soaked in deionized water. These slides were then placed in 70% ethanol for 2 minutes, followed by 90% ethanol for 2 minutes, 100% ethanol for 2 minutes, and xylene for 5 minutes. Cytoseal™ 60 mounting media with a coverslip was used for sealing the slides.

For the Oil Red O stain, duplicate slides were fixed in 10% neutral buffered formalin for 30 minutes. The slides were rinsed with deionized water and then stained in premade Mayer's hematoxylin stain for 20 minutes. These were rinsed again in deionized water, followed by soaking in 100% propylene glycol for 3 minutes to remove excess water. Preheated Oil Red O solution (0.5 g Oil Red O + 100 mL propylene glycol) was used for staining the slides for 20 minutes. A 2-minute soak in an 85% propylene glycol solution allowed for differentiation, followed by a final rinse with deionized water. Coverslips were placed on slides and sealed along the edges with nail polish.

Imaging was performed using a ZEISS Axio Imager 2 microscope. Fiber cross-sectional area (CSA) was measured on images taken from H&E stained slides using ZEN 2 (blue edition)

image-processing and analysis software. A total of 30-40 fibers from at least three different fields of view were measured for each sample (i.e. each tongue location). The circumference of each fiber was traced by hand, and the CSA was computed by the software.

3.7. Fiber type composition

Adenosine triphosphatase (ATPase) staining was performed to determine the percentage of type I (slow-twitch) and type II (fast-twitch) muscle fibers in beef tongue (Solomon & Dunn, 1988). Slides were rinsed with distilled water for 30 seconds before transferring to acid preincubation solution (50 mM potassium acetate, 18 mM $CaCl_2$, pH 4.15) for 8 minutes, followed by soaking twice in a Tris-$CaCl_2$ rinse solution (100 mM TRIS-HCl, 18 mM $CaCl_2$, pH 7.8). After soaking, slides were incubated in ATP media (0.1 M "221" Buffer, 2.7 mM ATP, 18 mM $CaCl_2$, 0.05 M KCl, pH 9.4) at 37 °C for 30 minutes. The slides were soaked in 1% $CaCl_2$, followed by 3 minutes in 2% (w/v) $CoCl_2$. After rinsing with distilled water, the slides were placed in 2% (v/v) ammonium sulfide for 3 minutes and finally rinsed in running tap water for 3 minutes. Cytoseal™ 60 mounting media with a coverslip was used for sealing the slides.

Imaging was performed using a ZEISS Axio Imager 2 microscope. Three fields of view were captured for each sample, and the number of dark (type I, slow-twitch) and light (type II, fast-twitch) fibers in each field of view was manually counted. These counts were totaled to calculate the percentage of slow-twitch and fast-twitch fibers in each sample.

3.8. Sarcomere length

Sarcomere length was measured according to the protocol of Weaver, Bowker, and Gerrard (2008). To prepare myofibrils for sarcomere length measurement, excess fat and connective tissue were trimmed from beef tongue before cutting and mincing. A 2 mg sample of the minced muscle was placed into a 50 mL centrifuge tube, with 14 mL of rigor buffer (75 mM

KCl, 10 mM imidazole, 2 mM $MgCl_2$, 2 mM EGTA, 1 mM NaN_3, pH 7.2) containing 0.5% Triton X-100. The sample was homogenized twice for 5 seconds and centrifuged at 1,000 *g* at 4 °C for 10 minutes. The supernatant was discarded. Another 14 mL of rigor buffer containing 0.5% Triton X-100 was added, and the tube was vortexed for 15 seconds and homogenized for 5 seconds. The samples were centrifuged again at 1,000 *g* at 4 °C for 10 minutes, and the supernatant was discarded. A 14 mL aliquot of rigor buffer without Triton X-100 was added to the sample, and the tubes were vortexed before a final centrifugation step was performed at 1,000 *g* at 4 °C for 10 minutes. The supernatant was discarded and the final pellet resuspended in 28 mL of rigor buffer.

To prepare slides for microscopy, 5 μL of the prepared myofibril homogenate and 75 μL of slide fixative were added to a clean slide coverslip and gently spread with a pipette tip. The coverslips were placed in a 35 °C oven for 10 minutes to dry, after which they were rinsed with deionized water. Mounting media (approximately 30 μL) was added to a clean slide, and the coverslip with homogenate was placed face down on the slide. The edges of the coverslip were sealed with fingernail polish and allowed to dry. A ZEISS Axio Imager 2 microscope with oil-immersion 100X objective was used to measure sarcomere lengths. For each sample, the lengths of 25-30 myofibrils, at least 5 sarcomeres long each, were measured using ZEN 2 (blue edition) image-processing and analysis software. Sarcomere length was calculated by dividing the myofibril length by number of sarcomeres.

3.9. Statistical analyses

All statistical analyses were performed using JMP Pro Version 14 software. One-way analysis of variance (ANOVA) was used to determine the statistical significance ($p<0.05$) of differences for fatty acid composition, proximate composition, and cross-sectional area (CSA)

between the regions of the tongue. Two-way ANOVA was used to determine the statistical significance ($p<0.05$) of differences in fiber type composition between the regions as well as the surface and interior muscles. The means of all analyses were compared using Tukey's honestly significant difference (HSD) test.

CHAPTER 4

RESULTS

4.1. Proximate composition

Proximate composition analysis of beef tongue revealed differences in moisture, protein, fat, and ash content along the length of the tongue (Table 1). Moisture content decreased progressively from the anterior region to the posterior. The moisture content was higher ($p<0.05$) in the anterior and anteromedial regions compared with the posteromedial and posterior regions. Crude protein content also decreased progressively from the anterior to the posterior region. On a dry-basis (db), the protein content was higher ($p<0.05$) in the anterior region than the anteromedial, posteromedial, and posterior regions. The highest protein content was in the anterior region (85.8% db), and the lowest was in the posterior region (36.1% db). Conversely, fat content increased from the anterior region to the posterior. The anterior and anteromedial regions exhibited lower ($p<0.05$) percent fat values than the posteromedial and posterior regions. When analyzed at $p<0.1$, the dry-basis percent fat value is lower in the anterior region than in the anteromedial region ($p=0.0634$). On a dry-basis, the lowest value of percent fat was in the anterior region (7.2% db), and the highest was in the posterior region (58.6% db). Ash content decreased from anterior to posterior, although ash composed a much smaller portion of the muscle overall than fat and protein. On a dry-basis, the ash content was higher ($p<0.05$) in the anterior region of the tongue than the posteromedial and posterior. The ash content ranged from 4.7% (db) in the anterior region to 2.5% (db) in the posterior.

4.2. Protein analyses

SDS-PAGE separations of the myofibrillar and sarcoplasmic protein fractions of beef tongue, *L. dorsi*, and beef heart muscle are shown in Figure 2. Together these two fractions represent the protein profile. The band patterns resulting from the separations reveal that beef tongue has a protein profile distinct from both *L. dorsi* and heart muscles. The myosin and actin bands are the most prominent bands observed in the myofibrillar fractions of all samples; these bands are indicated by arrows in Figure 2. Myoglobin, indicated by an arrow in Figure 2, was identified in all sarcoplasmic fractions and appears to be present at relatively similar concentrations. The band pattern seen in the myofibrillar fraction of beef tongue more closely resembles that of *L. dorsi* than that of heart. However, beef tongue's sarcoplasmic fraction band pattern is distinct from that of *L. dorsi*. It more closely resembles that of heart than that of *L. dorsi*.

LC-MS/MS analysis of the sarcoplasmic protein fraction of beef tongue muscle identified 262 proteins. Analysis of the sarcoplasmic protein fraction *L. dorsi* identified 161 proteins. A total of 157 of these proteins were found in both samples. Proteins known to be involved in cellular respiration were selected, and their abundance in each fraction, given by peak area, is summarized in Table 2. The analysis revealed a higher abundance of myoglobin in beef tongue than *L. dorsi*, with peak areas of 3.2×10^9 and 1.8×10^9, respectively. Both the cytoplasmic and mitochondrial types of creatine kinase were also more abundant in beef tongue than *L. dorsi*.

Of the proteins involved in glycolysis, glucose-6-phosphate isomerase, ATP-dependent 6-phosphofructokinase, glyceraldehyde-3-phosphate dehydrogenase, and L-lactate dehydrogenase were more abundant in beef tongue than *L. dorsi*. Conversely, fructose-

bisphosphate aldolase, phosphoglycerate kinase, phosphoglycerate mutase, and α- and β-enolase were more abundant in *L. dorsi* than beef tongue.

All TCA cycle proteins identified in the samples were more abundant in beef tongue compared with *L. dorsi*, including some proteins which were not detected in the *L. dorsi* fraction. Pyruvate dehydrogenase (β subunit), citrate synthase, isocitrate dehydrogenase, glutamate dehydrogenase 1, the 2-oxoglutarate dehydrogenase complex, the succinyl-CoA synthetase complex, and succinate dehydrogenase were abundant in the beef tongue fraction, but undetected in the *L. dorsi* fraction. Other mitochondrial proteins, including cytochrome *c* and ubiquinone biosynthesis protein COQ9, were also undetected in *L. dorsi* but abundant in beef tongue. All of the mitochondrial proteins detected in both samples were more abundant in beef tongue than *L. dorsi*. These include ATP synthase (α and β subunits), acetyl-CoA acetyltransferase, and aspartate aminotransferase.

4.3. Fatty acid profile

Fatty acid analyses revealed differences in the content of saturated fatty acids (SFAs), monounsaturated fatty acids (MUFAs), and polyunsaturated fatty acids (PUFAs) along the length of the tongue (Table 3). PUFAs constituted a smaller percent of fatty acids in all regions of the tongue, compared with MUFAs and SFAs. However, the PUFA content in the anterior region of the tongue was higher ($p<0.05$) than in the medial and posterior regions. The anterior region had an average of 13.0% polyunsaturation, whereas the medial and posterior regions had averages of 6.2% and 5.3%, respectively. Conversely, the SFA content was lower ($p<0.05$) in the anterior region of the tongue than in the posterior region. The anterior region had an average of 40.7% saturation, while the medial and posterior regions had averages of 48.1% and 50.5%, respectively. When analyzed at $p<0.1$, the SFA content in the anterior region is also lower than

the medial region (p=0.0622). The anterior region exhibited numerically higher values for MUFA content compared with the medial and posterior regions, but the values were not statistically different (p<0.05).

The percent composition of individual fatty acids for each sample is shown in Table 4. Oleic acid (C18:1 n-9) made up the greatest percent composition of the fatty acids in all samples, representing about 33.7% (± 2.7%). Palmitic acid (C16:0) and stearic acid (C18:0) composed the second and third greatest percentages in all samples, with overall averages of 23.9% ± 3.2% and 16.3% ± 1.8%, respectively.

4.4. Histological analyses

Hematoxylin and eosin (H&E) staining allowed for visualization of the basic tissue structure of beef tongue muscle. The shape and size of individual muscle fibers and fiber bundles can be observed. In Figure 3, adjacent fiber bundles are observed intersecting at right angles and running in perpendicular directions. Longitudinal and transverse fibers are indicated by arrows. Changes in fiber direction are more frequent in the interior section of the tongue than in the surface, as observed in Figure 4. Groups of fiber bundles running in opposite directions intersect each other more often in the tongue's interior compared with the tongue's surface, where groups of bundles running in the same direction are less frequently interrupted by perpendicular fiber bundles. Images A, C, and E of Figure 4 were taken from the surface, where the majority of fibers run in the same direction. Images B, D, and F were taken from the interior, where perpendicular fiber bundles are more interspersed.

Masson's trichrome staining highlighted the connective tissue structure of beef tongue. Connective tissue can be seen surrounding individual muscle fibers (endomysium), fiber bundles (perimysium), and groups of fiber bundles (epimysium) as indicated by arrows in Figure 5. The

perimysium is thicker than the endomysium, and the epimysium is thicker than both the perimysium and the endomysium.

Oil Red O staining allowed for differentiation of fat cells in the beef tongue muscle. Lipids were observed as pockets between muscle fiber bundles. The amount of fat increases from the anterior to the posterior region of the tongue, which is shown in Figure 6. Image A was taken from the anterior, B from the medial, and C from the posterior region. The higher lipid content in the posterior region compared to the anterior region can also be seen by the naked eye when dissecting the tongue (Figure 7). Fat was observed to accumulate in the interior of the tongue, with less fat being present towards the surface. This accumulation can be seen in Figure 7, with the interior and surface areas indicated by arrows, as well as in Figure 8. Images A, C, and E of Figure 8 were taken from the tongue's surface, while images B, D, and F were taken from the interior.

The average sarcomere lengths of four beef tongue samples are displayed in Table 5. The anterior region had an average sarcomere length of 2.25 ± 0.29 μm, and the posterior had an average length of 2.17 ± 0.28 μm. All samples had an average sarcomere length greater than 2 μm. Average cross-sectional areas (CSA) of muscle fibers in the anterior, medial, and posterior regions of beef tongue are also displayed in Table 5. Muscle fibers in the anterior region of the tongue exhibited higher (p<0.05) CSA than the medial and posterior regions. Fibers in the medial region exhibited the lowest (p<0.05) CSA of the three regions.

4.5. Fiber type composition

ATPase staining revealed the percentage of type I and type II muscle fibers in beef tongue. Table 6 shows the percentage of each fiber type in the anterior, medial, and posterior regions of the tongue, with the muscles of each region separated into interior and surface. The

majority of fibers in all samples are type I, except in the surface muscles of the anterior region. The percentage of type I fibers is highest in the posterior region, with 75.0 and 74.5% type I fibers in the surface and interior, respectively. The surface muscles of the anterior region are the only location with a majority of type II fibers; only 39.2% were type I fibers. The difference in fiber type proportion between the anterior and posterior region can be seen in Figure 9. In the anterior and medial regions, the interior muscles had a higher percentage of type I fibers than the surface muscles. In the medial region, the interior had 64.7% type I fibers and the surface had 55.7%. In the anterior region, the interior had 63.0% type I fibers and the surface had 39.2%. The difference in fiber type proportion between the surface and interior is shown in Figure 10.

A high level of variability was observed between muscle bundles. Within a single sample, some bundles had very different proportions of dark and light fibers than others, even between adjacent bundles. This variability is shown in Figure 11.

CHAPTER 5

DISCUSSION

The primary objective of this study was to evaluate and characterize the physicochemical composition of beef tongue. Proximate composition analysis revealed that beef tongue has a higher concentration of fat in the posterior region than the anterior. A GC-FID analysis confirmed this finding and determined that the MUFA oleic acid (C18:1 n-9) is the dominant fatty acid in beef tongue. These results are in agreement with a study by Siedler, Springer, Slover, & Kizlaitis (1964). They found that oleic acid made up to 44% of the total fatty acid content of beef tongue. Oleic acid is an essential fatty acid known for its health benefits (Lopez-Huertas, 2010). These findings suggest that beef tongue has high nutritional value as a source of healthy fatty acids. The analysis also showed that the anterior region has higher PUFA and lower SFA content than the posterior. It is logical that the anterior region of the tongue is the healthiest portion for consumption.

In addition, proximate composition analysis showed that the protein and ash content of beef tongue is higher in the anterior region than the posterior. The USDA Food Composition Database cites that beef tongue provides 14.78 g protein, 2.93 mg iron, 2.85 mg zinc, and 3.76 mg vitamin B_{12} per 3.5 ounce serving ("Full Report (All Nutrients) 13339, Beef, variety meats and by-products, tongue, raw," 2018). The results of the present study indicate that a higher concentration of this nutritional content is found in the anterior region of the tongue than the posterior.

The results of SDS-PAGE separation of myofibrillar protein fractions indicate that the myofibrillar protein content of beef tongue is more similar to that of *L. dorsi* than heart. Both *L. dorsi* and tongue are skeletal muscles, while heart is a cardiac muscle, so the contraction of tongue myofibrils would be expected to be more similar to that of *L. dorsi* than heart. Conversely, the results of sarcoplasmic protein fraction separation suggest that beef tongue is metabolically more similar to heart than *L. dorsi*. The heart is a muscle that is constantly working and thus relies exclusively on aerobic metabolism (Voet et al., 2006). The similarity between beef tongue and heart sarcoplasmic protein profiles indicates that the metabolism of tongue may also be primarily aerobic.

The data from LC-MS proteomic analysis and fiber typing provide further indication that beef tongue relies more on oxidative metabolic pathways than glycolytic to meet its energy demands. A comparison of the proteins detected by LC-MS analysis of beef tongue and *L. dorsi* sarcoplasmic protein fractions indicates that tongue relies more on oxidative metabolism than *L. dorsi*. Studies have reported that *L. dorsi*. is composed of a majority of white fibers and thus relies primarily on glycolytic metabolism (Kirchofer, Calkins, & Gwartney, 2002). The data reveal a higher abundance of both myoglobin and creatine kinase in beef tongue than *L. dorsi*. The higher abundance of myoglobin suggests a higher oxygen requirement for beef tongue than *L. dorsi*. Creatine kinase is an enzyme involved in maintaining ATP supply for cells with high energy demands, so the higher abundance of creatine kinase in tongue suggests greater energy requirements for tongue than *L. dorsi* (McLeish & Kenyon, 2005). Enzymes involved in oxidative metabolic pathways had lower abundance in *L. dorsi* than tongue, including some which were undetected in *L. dorsi*. The higher abundance of oxidative metabolic enzymes in beef tongue suggests that it may have higher concentrations of mitochondria than *L. dorsi*. Further

research to isolate and quantify mitochondria in beef tongue, *L. dorsi*, and heart would serve to confirm this hypothesis.

The results of fiber typing corresponded with protein analysis in their indication that beef tongue relies primarily on oxidative metabolism. The majority of all fibers in the tongue were determined to be type I, oxidative fibers. This finding is in agreement with a study by Sanders, Mu, Amirali, Su, and Sobotka (2013) which determined 54% of fibers in the human tongue to be type I, slow-twitch. The highest proportion of type II fibers was found in the surface muscles of the anterior region of the tongue. This is likely due to the anterior performing quicker movements, with the posterior performing mostly slow, stabilizing movements which may be maintained for long periods of time. A study by Stål, Marklund, Thornell, De Paul, and Eriksson (2003) similarly found the human tongue to have a higher proportion of type II fibers in the anterior region than the posterior. The tongue's interior muscles were found to have a higher proportion of type I fibers than the surface muscles. This could be due to the interior muscles being responsible for stabilizing the tongue and sustaining muscle movements. Past research has found that meat tenderness and juiciness is improved with increased proportions of type I fibers, so the data can be interpreted to suggest that beef tongue is likely to improve these qualities in a meat product (Hwang, Kim, Jeong, Hur, & Joo, 2010; Strydom, Naude, Smith, Scholtz, & van Wyk, 2000; Listrat et al., 2016).

A prominent characteristic of beef tongue muscles observed by histological analysis was the high level of variability in orientation, size, and fiber type of muscle fibers, even in adjacent muscle bundles. H&E staining revealed an overlapping and interweaving pattern of fibers, particularly in the interior muscles. Groups of muscle bundles running parallel to each other were frequently seen intersected by adjacent bundles running perpendicularly. Additionally, the

bundles tended to be of irregular shape and size. Sanders and Mu (2013) studied the muscle structure of human tongue and also observed this arrangement of interweaving muscles. These patterns may be due to the complexity of movements the tongue is capable of performing.

Increased sarcomere length up to 2.0 μm has been shown to be correlated with increased tenderness (Wheeler, Shackelford, & Koohmaraie, 2000; Rhee, Wheeler, Shackelford, & Koohmaraie, 2004). The average sarcomere length of beef tongue determined in this study falls above this benchmark, suggesting that beef tongue may be expected to provide a tender meat product. Studies have also shown fiber CSA to be negatively correlated to meat tenderness (Listrat et al., 2016; Joo, Kim, Hwang, & Ryu, 2013; Seideman, Koohmaraie, & Crouse, 1988). In the present study, the medial region was found to have the smallest CSA, and thus it is expected to provide the most tender meat. The anterior region was found to have the largest CSA, which corresponds with the finding that it is also the most glycolytic region. Previous research has found glycolytic fibers to be larger on average than oxidative fibers (van Wessel, de Haan, van der Laarse, & Jaspers, 2010; van der Laarse, des Tombe, Lee-de Groot, & Diegenbach, 1998).

The data obtained through this study provide information on the physicochemical composition and muscular structure of beef tongue. This information can be used to capitalize on its potential as a value-added meat product. Future research on beef tongue should focus on exploring and evaluating possible applications for value addition in the food and meat industries. These applications will increase the value of beef tongue for the meat industry and provide consumers with an affordable and nutritional meat product.

CHAPTER 6

CONCLUSIONS

Our findings indicate that the anterior region of beef tongue has higher protein and lower fat content than the posterior. The findings also show that the fat content of the anterior region is richer in polyunsaturated fatty acids and lower in saturated fatty acids than the posterior, and that the dominant fatty acid in beef tongue is the monounsaturated fatty acid oleic acid (C18:1 n-9). These conclusions indicate that beef tongue, particularly the anterior portion, has the potential to be developed into a value-added meat product with high-quality fat content.

The results of protein analysis and fiber typing show that beef tongue relies primarily on oxidative metabolism. The sarcoplasmic protein fraction of beef tongue has an abundance of mitochondrial proteins and enzymes involved in oxidative metabolic pathways, compared with other skeletal muscles. The majority of beef tongue muscle fibers are type I (slow-twitch) oxidative fibers. The surface of the anterior region of beef tongue is the only location where type II (fast-twitch) glycolytic fibers predominate. The interior portion of beef tongue tends to have higher proportions of type I fibers than the surface muscles, and the greatest proportion of type I fibers is located in the posterior region. Primarily oxidative muscles are abundant in mitochondria and are known for higher tenderness. The findings of this study therefore indicate that beef tongue is also likely to produce a tender meat product.

This study was undertaken to provide the meat industry with information on beef tongue's physicochemical composition in order to improve its application as a meat product and value-added food ingredient. Potential applications include the incorporation of beef tongue into

ground meat or sausage and its conversion into a spray-dried powder to be used as a protein-rich additive to stocks or stews. Future research should focus on exploring and evaluating these possible applications, including the resulting products' textural attributes, taste, flavor, water-binding capacity, water-holding capacity, emulsification, and gelation properties.

The thick outer layer of skin surrounding the muscle presents a challenge when preparing beef tongue. Currently, the recommended method for removing this layer involves boiling the tongue for 3-4 hours until it can be more easily separated and peeled. Exploring alternative methods for peeling the tongue, such as high-pressure processing, would be advantageous to the meat industry. Ultimately, increasing the consumption of beef tongue will increase the economic incentives for the meat industry and provide consumers with an affordable and nutritional meat product.

REFERENCES

Alao, B., Falowo, A., Chulayo, A., & Muchenje, V. (2017). The potential of animal by-products in food systems: production, prospects and challenges. *Sustainability, 9*(7), 1089.

Biesalski, H. K. (2005). Meat as a component of a healthy diet - are there any risks or benefits if meat is avoided in the diet? *Meat Science, 70*(3), 509-524.

Boland, M. J., Rae, A. N., Vereijken, J. M., Meuwissen, M. P. M., Fischer, A. R. H., van Boekel, M. A. J. S., . . . Hendriks, W. H. (2013). The future supply of animal-derived protein for human consumption. *Trends in Food Science & Technolgy, 29*, 62-73.

Chan, J. K. C. (2014). The wonderful colors of the hematoxylin-eosin stain in diagnostic surgical pathology. *International Journal of Surgical Pathology, 22*(1), 12-32.

Christoffersen, S. D., & Thomsen, J. L. (2014). Can examination of tissue stained with Oil red O be postponed up to three months? *Scandinavian Journal of Forensic Science, 20*(2), 50-52.

Corbin, J. E. (1992). Inedible meat, poultry and fish by-products in pet foods. *Inedible meat by-products.* (Vol. 8, pp. 329-347). Dordrecht, Netherlands: Springer.

Doerscher, D. R., Briggs, J. L., & Lonergan, S. M. (2004). Effects of pork collagen on thermal and viscoelastic properties of purified porcine myofibrillar protein gels. *Meat Science, 66*(1), 181-188.

Ertbjerg, P., & Puolanne, E. (2017). Muscle structure, sarcomere length and influences on meat quality: A review. *Meat Science, 132*, 139-152.

Full Report (All Nutrients) 13339, Beef, variety meats and by-products, tongue, raw. (2018). Available from USDA National Nutrient Database for Standard Reference. Retrieved 02/07/2019 https://ndb.nal.usda.gov/ndb/foods/show/13339?n1=%7BQv%3D1%7D&fgcd=&man=&lfacet=&count=&max=25&sort=default&qlookup=beef+tongue&offset=&format=Full&new=&measureby=&Qv=1&ds=&qt=&qp=&qa=&qn=&q=&ing=

Goll, D. E., Young, R. B., & Stromer, M. H. (1974). Separation of subcellular organelles in differential and density gradient centrifugation. *Proceedings of the Reciprocal Meat Conference, 37*, 250-290.

Gong, Y., Pegg, R. B., Carr, E. C., Parrish, D. R., Kellett, M. E., & Kerrihard, A. L. (2017). Chemical and nutritive characteristics of tree nut oils available in the US market. *European Journal of Lipid Science and Technology, 119*(8), 1600520.

Gonulalan, Z., Kose, A., & Yetim, H. (2004). Effects of liquid smoke on quality characteristics of Turkish standard smoked beef tongue. *Meat Science, 66*(1), 165-170.

How to Feed the World in 2050. (2009). Rome; Italy: Food and Agriculture Organization of the United Nations (FAO).

Hwang, Y.-H., Kim, G.-D., Jeong, J.-Y., Hur, S.-J., & Joo, S.-T. (2010). The relationship between muscle fiber characteristics and meat quality traits of highly marbled Hanwoo (Korean native cattle) steers. *Meat Science, 86*(2), 456-461.

Jayathilakan, K., Sultana, K., Radhakrishna, K., & Bawa, A. S. (2012). Utilization of byproducts and waste materials from meat, poultry and fish processing industries: a review. *Journal of Food Science and Technology, 49*(3), 278-293.

Joo, S. T., Kim, G. D., Hwang, Y. H., & Ryu, Y. C. (2013). Control of fresh meat quality through manipulation of muscle fiber characteristics. *Meat Science, 95*(4), 828-836.

Kincs, F. (1985). Meat fat formulation. *Journal of the American Oil Chemists' Society, 62*(4), 815-818.

Listrat, A., Lebret, B., Louveau, I., Astruc, T., Bonnet, M., Lefaucheur, L., . . . Bugeon, J. (2016). How muscle structure and composition influence meat and flesh quality. *The Scientific World Journal, 2016*, 1-14.

Lopez-Huertas, E. (2010). Review: Health effects of oleic acid and long chain omega-3 fatty acids (EPA and DHA) enriched milks. A review of intervention studies. *Pharmacological Research, 61*(3), 200-207.

Market access triggers swings in beef variety meat values. (2013). Retrieved 03/12/2019, from U.S. Meat Export Federation http://proxy-remote.galib.uga.edu/login?url=http://search.ebscohost.com/login.aspx?direct=true&db=edsgin&AN=edsgcl.338009423&site=eds-live

Marti, D. M., Johnson, R. J., & Mathews, K. H. (2011). *Where's the (not) meat?- Byproducts from beef and pork production* (LDP-M-209-01). Washington, D.C.: United States Department of Agriculture, Economic Research Service. Retrieved from https://www.ers.usda.gov/webdocs/publications/37427/8801_ldpm20901.pdf?v=0.

Martinello, T., Pascoli, F., Caporale, G., Perazzi, A., Iacopetti, I., & Patruno, M. (2015). Might the Masson trichrome stain be considered a useful method for categorizing experimental tendon lesions? *Histology and Histopathology, 30*(8), 963-969.

Miller, M. F., Keeton, J. T., Cross, H. R., Leu, R., Gomez, F., & Wilson, J. J. (1988). Evaluation of the physical and sensory properties of jerky processed from beef heart and tongue. *Journal of Food Quality, 11*(1), 63-70.

Nollet, L. M. L., & Toldrá, F. (2011). *Handbook of analysis of edible animal by-products*. Boca Raton, FL: CRC Press.

Ockerman, H. W., & Hansen, C. L. (2000). *Animal by-product processing & utilization*. Lancaster, PA: CRC Press.

Pearson, A. M., & Young, R. B. (1989). *Muscle and meat biochemistry*. San Diego, CA: Academic Press, Inc.

Rhee, M. S., Wheeler, T. L., Shackelford, S. D., & Koohmaraie, M. (2004). Variation in palatability and biochemical traits within and among eleven beef muscles. *Journal of Animal Science, 82*(2), 534-550.

Sanders, I., & Mu, L. (2013). A three-dimensional atlas of human tongue muscles. *The Anatomical Record, 296*, 1102-1114.

Sanders, I., Mu, L., Amirali, A., Su, H., & Sobotka, S. (2013). The human tongue slows down to speak: muscle fibers of the human tongue. *The Anatomical Record, 296*(10), 1615-1627.

Schaefer, D., & Arp, T. (2017). Importance of variety meat utilization to the meat industry. *Animal Frontiers, 7*(4), 25-28.

Seideman, S. C., Koohmaraie, M., & Crouse, J. D. (1988). The influence of muscle fiber size on tenderness in A-maturity heifers. *Journal of Food Quality, 11*(1), 27-34.

Siedler, A. J., Springer, D., Slover, H. T., & Kizlaitis, L. (1964). Nutrient content of variety meats. III. Fatty acid composition of lipids of certain raw and cooked variety meats. *Journal of Food Science, 29*(6), 877-880.

Solomon, M. B., & Dunn, M. C. (1988). Simultaneous histochemical determination of three fiber types in single sections of ovine, bovine and porcine skeletal muscle. *Journal of Animal Science, 66*(1), 255-264.

Stål, P., Marklund, S., Thornell, L. E., De Paul, R., & Eriksson, P. O. (2003). Fibre composition of human intrinsic tongue muscles. *Cells, Tissues, Organs, 173*(3), 147-161.

Strydom, P. E., Naude, R. T., Smith, M. F., Scholtz, M. M., & van Wyk, J. B. (2000). Characterization of indigenous African cattle breeds in relation to carcass characteristics. *Meat Science, 55*(1), 79-88.

Tao, L. (2015). Oxidation of polyunsaturated fatty acids and its impact on food quality and human health. *Advances in Food Technology and Nutritional Sciences, 1*(6), 135-142.

Toldrá, F., Aristoy, M. C., Mora, L., & Reig, M. (2012). Innovations in value-addition of edible meat by-products. *Meat Science, 92*(3), 290-296.

Vahmani, P., Mapiye, C., Prieto, N., Rolland, D. C., McAllister, T. A., Aalhus, J. L., & Dugan, M. E. R. (2015). The scope for manipulating the polyunsaturated fatty acid content of beef: a review. *Journal of Animal Science and Biotechnology, 6*(1), 1-13.

van der Laarse, W. J., des Tombe, A. L., Lee-de Groot, M. B. E., & Diegenbach, P. C. (1998). Size principle of striated muscle cells. *Netherlands Journal of Zoology, 48*(3), 213-223.

Van Elswyk, M. E., & McNeill, S. H. (2014). Impact of grass/forage feeding versus grain finishing on beef nutrients and sensory quality: The U.S. experience. *Meat Science, 96*(1), 535-540.

van Wessel, T., de Haan, A., van der Laarse, W. J., & Jaspers, R. T. (2010). The muscle fiber type-fiber size paradox: hypertrophy or oxidative metabolism? *European Journal of Applied Physiology, 110*(4), 665-694.

Vanderzant, C., Hanna, M. O., Ehlers, J. G., Savell, J. W., Griffin, D. B., Johnson, D. D., . . . Stiffler, D. M. (1985). Methods of chilling and packaging of beef, pork and lamb variety meats for transoceanic shipment: microbiological characteristics. *Journal of Food Protection, 48*(9), 765-769.

Visser, I. J. R., Koolmees, P. A., & Bijker, P. G. H. (1988). Microbiological conditions and keeping quality of veal tongues as affected by lactic acid decontamination and vacuum packaging. *Journal of Food Protection, 51*(3), 208-213.

Voet, D., Voet, J. G., & Pratt, C. W. (2006). *Fundamentals of biochemistry: Life at the molecular level* (2nd ed.). Hoboken, NJ: John Wiley & Sons, Inc.

Weaver, A. D., Bowker, B. C., & Gerrard, D. E. (2008). Sarcomere length influences postmortem proteolysis of excised bovine semitendinosus muscle. *Journal of Animal Science, 86*(8), 1925-1932.

Wheeler, T. L., Shackelford, S. D., & Koohmaraie, M. (2000). Variation in proteolysis, sarcomere length, collagen content, and tenderness among major pork muscles. *Journal of Animal Science, 78*(4), 958-965.

Wood, J. D., Enser, M., Fisher, A. V., Nute, G. R., Sheard, P. R., Richardson, R. I., . . . Whittington, F. M. (2008). Fat deposition, fatty acid composition and meat quality: A review. *Meat Science, 78*(4), 343-358.

Table 1. Proximate composition of beef tongue

Tongue Region*	Moisture	Protein	Fat	Ash
		% (Wet-Basis)		
Anterior	77.6 ± 0.7^{a}	19.2 ± 1.3^{a}	1.6 ± 0.9^{b}	1.1 ± 0.0^{a}
Anteromedial	73.1 ± 4.0^{a}	17.8 ± 2.3^{a}	7.5 ± 5.5^{b}	1.0 ± 0.1^{a}
Posteromedial	66.8 ± 3.4^{b}	15.9 ± 1.5^{b}	16.1 ± 4.9^{a}	1.0 ± 0.1^{a}
Posterior	61.2 ± 4.0^{b}	13.8 ± 1.2^{c}	22.9 ± 4.6^{a}	1.0 ± 0.1^{a}
		% (Dry-Basis)		
Anterior	-	85.8 ± 7.9^{a}	7.2 ± 3.9^{b}	4.7 ± 0.1^{a}
Anteromedial	-	68.0 ± 17.2^{b}	26.3 ± 15.7^{b}	3.9 ± 0.7^{ab}
Posteromedial	-	48.6 ± 9.8^{c}	47.9 ± 10.4^{a}	2.9 ± 0.5^{bc}
Posterior	-	36.1 ± 7.1^{c}	58.6 ± 6.6^{a}	2.5 ± 0.5^{c}

*Denotes the location/region where each sample was taken from the tongue. See Figure 1 for a diagram of sampling regions. Numbers in a column with different letters (*a*-*c*) are statistically different ($p<0.05$).

Table 2. Comparison of proteins identified in beef tongue and *Longissimus dorsi*

Protein		Peak Area	
		Tongue	*L. dorsi*
Myoglobin		3.2×10^{9}	1.8×10^{9}
Creatine Kinase			
	*M-type**	3.1×10^{9}	1.8×10^{9}
	*S-type**	5.4×10^{8}	3.4×10^{7}
Glucose-6-phosphate isomerase		1.6×10^{8}	1.4×10^{8}
ATP*-dependent 6-phosphofructokinase		5.2×10^{7}	2.9×10^{7}
Fructose-bisphosphate aldolase		1.5×10^{8}	2.5×10^{8}
Glyceraldehyde-3-phosphate dehydrogenase		3.0×10^{9}	2.3×10^{9}
Phosphoglycerate kinase		1.9×10^{8}	2.7×10^{8}
Phosphoglycerate mutase			
	*1**	1.2×10^{8}	3.6×10^{8}
	*2**	6.0×10^{8}	9.9×10^{8}
α-enolase		1.6×10^{8}	2.9×10^{8}
β-enolase		4.7×10^{8}	1.2×10^{9}
L-lactate dehydrogenase			
	*A chain**	7.5×10^{8}	5.0×10^{8}
	*B chain**	8.0x10^{8}	4.6×10^{8}
Pyruvate dehydrogenase (E1)			
	*α subunit**	1.6×10^{7}	2.8×10^{6}
	β *subunit**	2.6×10^{7}	0
Citrate synthase		7.4×10^{7}	0
Aconitase		1.4×10^{8}	1.5×10^{7}
Isocitrate dehydrogenase		5.8×10^{7}	0
Glutamate dehydrogenase 1		9.9×10^{6}	0
2-Oxoglutarate dehydrogenase complex			
	*E1**	2.5×10^{6}	0
	*E2**	1.0×10^{7}	0
Succinate-CoA ligase			
	ADP-forming*	6.5×10^{6}	0
	GDP-forming*	1.5×10^{7}	0
Succinate dehydrogenase			
	*α subunit**	2.3×10^{7}	0
	β *subunit**	2.2×10^{7}	0
Malate dehydrogenase			
	*Mitochondrial**	2.8×10^{8}	3.3×10^{7}
	*Cytoplasmic**	5.7×10^{8}	7.4×10^{7}

Ubiquinone biosynthesis protein COQ9		9.0×10^6	0
Cytochrome *c*		5.0×10^7	0
ATP* synthase			
	α subunit	1.9×10^7	2.1×10^6
	β *subunit*	1.8×10^8	8.1×10^6
	γ subunit	1.4×10^6	0
	δ subunit	1.8×10^7	0
Acetyl-CoA acetyltransferase		2.7×10^7	1.9×10^6
3-ketoacyl-CoA thiolase		1.6×10^7	0
Very long-chain specific acyl-CoA dehydrogenase		1.5×10^7	0
Medium-chain specific acyl-CoA dehydrogenase		2.2×10^7	0
Short-chain specific acyl-CoA dehydrogenase		1.3×10^7	0
Enoyl-CoA hydratase		1.1×10^7	0
Aspartate aminotransferase		8.0×10^7	7.1×10^6
3-hydroxyisobutyrate dehydrogenase		5.7×10^6	0
Isovaleryl-CoA dehydrogenase		9.4×10^6	0
ATPase inhibitor		2.1×10^7	9.1×10^6
Adenylate kinase 2		1.1×10^7	0
Aldehyde dehydrogenase		9.2×10^6	3.1×10^6
NAD*-dependent protein deacylase sirtuin-5		3.2×10^6	0
NAD(P)H*-hydrate epimerase		5.4×10^6	0
GTP:AMP* phosphotransferase (adenylate kinase 3)		1.1×10^7	0

Proteins were identified by LC-MS/MS.

*Creatine kinase M-type refers to the cytoplasmic isoenzyme. S-type refers to the mitochondrial isoenzyme.

Phosphoglycerate mutase 1 refers to the ubiquitous form of the enzyme. Phosphoglycerate mutase 2 is the muscle-specific form.

L-lactate dehydrogenase A and B chains are two subunits of the enzyme.

Pyruvate dehydrogenase (E1) α and β subunits form the heterotetramer structure of the enzyme.

E1 of the 2-oxoglutarate dehydrogenase complex refers to 2-oxoglutarate dehydrogenase. E2 of the complex refers to dihydrolipoyllysine-residue succinyltransferase.

Succinate dehydrogenase α and β subunits refer to the two subunits that make up the heterodimeric electron transfer flavoprotein.

Mitochondrial and cytoplasmic malate dehydrogenase refer to the two main isoforms of the enzyme.

ATP synthase subunits α, β, γ, and δ are subunits of the F_1 domain.

ATP= adenosine triphosphate

ADP= adenosine diphosphate

AMP= adenosine monophosphate

GTP= guanosine triphosphate

GDP= guanosine diphosphate

NAD= nicotinamide adenine dinucleotide

NAD(P)H= nicotinamide adenine dinucleotide (phosphate), reduced form

Table 3. Composition of saturated, monounsaturated, and polyunsaturated fatty acids in beef tongue

Tongue Region*	Saturated Fatty Acids (%)	Monounsaturated Fatty Acids (%)	Polyunsaturated Fatty Acids (%)
Anterior	40.7^{b}	46.3^{a}	13.0^{a}
Medial	48.1^{ab}	45.7^{a}	6.2^{b}
Posterior	50.5^{a}	44.1^{a}	5.3^{b}

*Denotes the location/region where each sample was taken from the tongue. See Figure 1 for a diagram of sampling regions. Numbers in a column with different letters (*a*-*b*) are statistically different ($p<0.05$).

Table 4. Fatty acid composition of beef tongue

	Average % Composition by Region*		
Fatty Acid	Anterior	Medial	Posterior
C6:0	0.2 ± 0.0	0.1 ± 0.0	0.1 ± 0.0
C8:0	0.1 ± 0.1	0.0 ± 0.0	0.0 ± 0.0
C10:0	0.1 ± 0.0	0.1 ± 0.0	0.1 ± 0.0
C12:0	0.1 ± 0.0	0.1 ± 0.0	0.1 ± 0.0
C14:0	2.2 ± 0.5	5.8 ± 4.0	4.0 ± 1.7
C14:1n-5	0.4 ± 0.1	0.6 ± 0.2	0.5 ± 0.1
C15:0	0.7 ± 0.0	0.9 ± 0.1	1.0 ± 0.1
C15:1	0.2 ± 0.1	0.0 ± 0.0	0.0 ± 0.0
C16:0	20.1 ± 0.5	24.6 ± 2.4	26.9 ± 0.9
C16:1n-9	0.8 ± 0.0	0.8 ± 0.2	0.9 ± 0.0
C16:1n-7	6.4 ± 4.7	3.8 ± 0.6	3.3 ± 0.5
C17:1	1.5 ± 0.2	1.3 ± 0.2	1.2 ± 0.2
C18:0	15.9 ± 0.7	15.5 ± 2.2	17.4 ± 2.1
C18:1 Trans	3.0 ± 0.4	3.2 ± 0.4	2.2 ± 0.8
C18:1n-9	31.7 ± 1.8	34.2 ± 3.2	35.0 ± 2.6
C18:1n-7	2.1 ± 0.3	1.7 ± 0.2	1.0 ± 0.5
C18:2n-6	5.9 ± 0.9	3.4 ± 0.7	2.9 ± 0.5
C20:0	0.1 ± 0.0	0.1 ± 0.0	0.1 ± 0.1
C18:3n-6 (GLA)	0.1 ± 0.0	0.1 ± 0.0	0.1 ± 0.0
C20:1n-9	0.1 ± 0.1	0.1 ± 0.0	0.1 ± 0.0
C18:3n-3 (ALA)	1.6 ± 0.1	1.1 ± 0.2	1.0 ± 0.1
C21:0	0.9 ± 0.1	0.8 ± 0.3	0.8 ± 0.1
C20:2n-6	0.1 ± 0.0	0.1 ± 0.0	0.1 ± 0.0
C22:0	0.2 ± 0.1	0.1 ± 0.0	0.1 ± 0.0
C18:3n-6 (DGLA)	0.6 ± 0.1	0.2 ± 0.1	0.1 ± 0.0
C20:3n-3 (ETE)	0.3 ± 0.2	0.2 ± 0.1	0.2 ± 0.1
C20:4n-6 (AA)	1.8 ± 0.9	0.3 ± 0.1	0.2 ± 0.0
C22:2n-6	0.2 ± 0.1	0.1 ± 0.1	0.1 ± 0.0
C24:0	0.0 ± 0.0	0.0 ± 0.0	0.0 ± 0.0
C20:5n-3 (EPA)	0.8 ± 0.5	0.1 ± 0.0	0.1 ± 0.0
C22:5n-3	1.4 ± 0.8	0.5 ± 0.2	0.5 ± 0.1
C22:6n-3 (DHA)	0.2 ± 0.1	0.1 ± 0.0	0.0 ± 0.0

*Denotes the location/region where each sample was taken from the tongue.

Table 5. Sarcomere length and fiber cross-sectional area of beef tongue

Tongue Region*	Sarcomere Length (μm) ± SDV	Cross-Sectional Area (μm^2)
Anterior	2.3 ± 0.3	2221.1^{a}
Medial	-	1574.8^{c}
Posterior	2.2 ± 0.3	1823.9^{b}

*Denotes the location/region where each sample was taken from the tongue. See Figure 1 for a diagram of sampling regions.
Sarcomere length was measured in samples taken from the anterior half and posterior half of the tongue.
Cross-sectional area: numbers with different letters (*a-c*) are statistically different ($p<0.05$).

Table 6. Percentage of type I and type II fibers in beef tongue

Tongue Region*	Type I (slow-twitch)		Type II (fast-twitch)	
	n*	%	n*	%
Anterior *surface*	230	39.2 ± 15.5^{b}	308	60.8 ± 15.5^{a}
Anterior *interior*	313	63.0 ± 10.4^{ab}	175	37.0 ± 10.4^{ab}
Medial *surface*	355	55.7 ± 11.7^{ab}	301	44.3 ± 11.7^{ab}
Medial *interior*	468	64.7 ± 11.1^{ab}	243	35.3 ± 11.1^{ab}
Posterior *surface*	444	75.0 ± 3.1^{a}	148	25.0 ± 3.1^{b}
Posterior *interior*	512	74.5 ± 5.7^{a}	179	25.5 ± 5.7^{b}

*Denotes the location/region where each sample was taken from the tongue. See Figure 1 for a diagram of sampling regions. n = number of fibers counted. Numbers in a column with different letters (*a*-*b*) are statistically different ($p<0.05$).

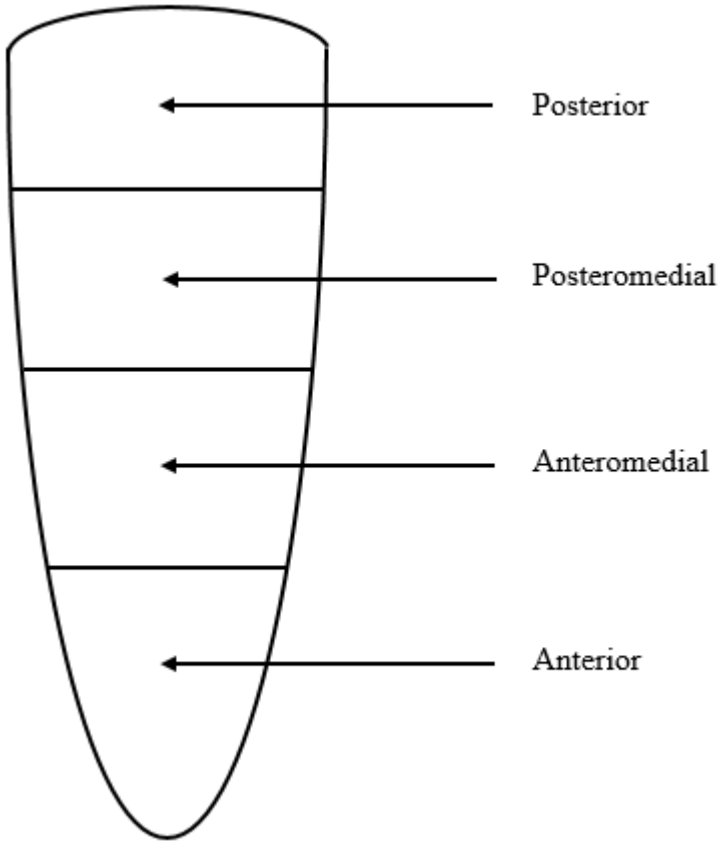

Figure 1. Diagrammatic representation of beef tongue regions for sampling. Samples denoted as being taken from the medial region combined material from the antero- and posteromedial regions.

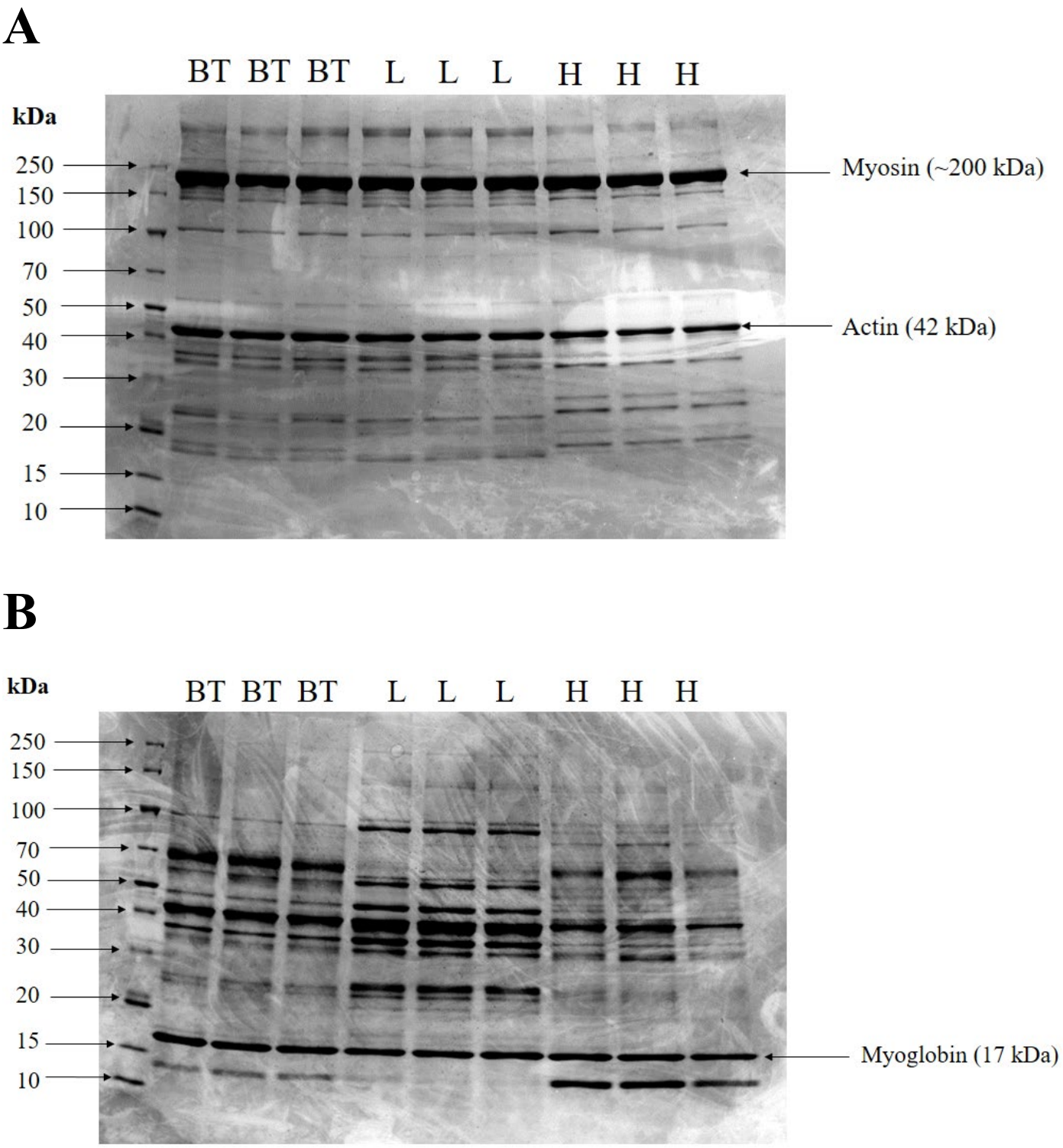

Figure 2. Coomassie-stained SDS-PAGE* gels of beef tongue (BT), *L. dorsi* (L), and heart (H) isolated protein fractions. **A**) myofibrillar fraction, **B**) sarcoplasmic fraction.
*SDS-PAGE= sodium dodecyl sulfate polyacrylamide gel electrophoresis.

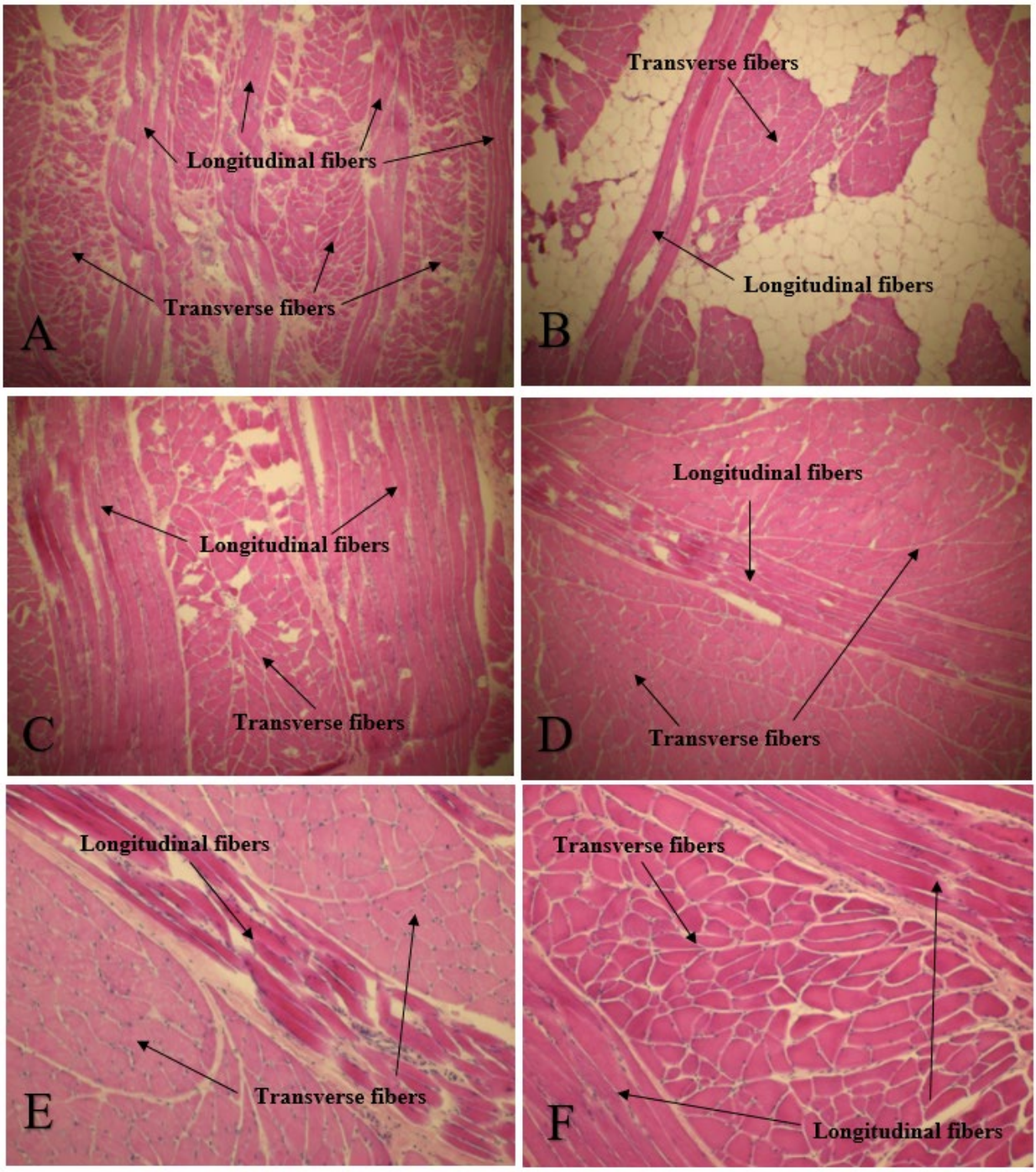

Figure 3. H&E staining of beef tongue muscle taken from **A)** and **F)** interior of the medial region, **B)** interior of the posterior region, **C)** interior of the anterior region, and **D)** and **E)** surface of the anterior region. Objective lens setting: **A-D)** 5x; **E-F)** 10x.

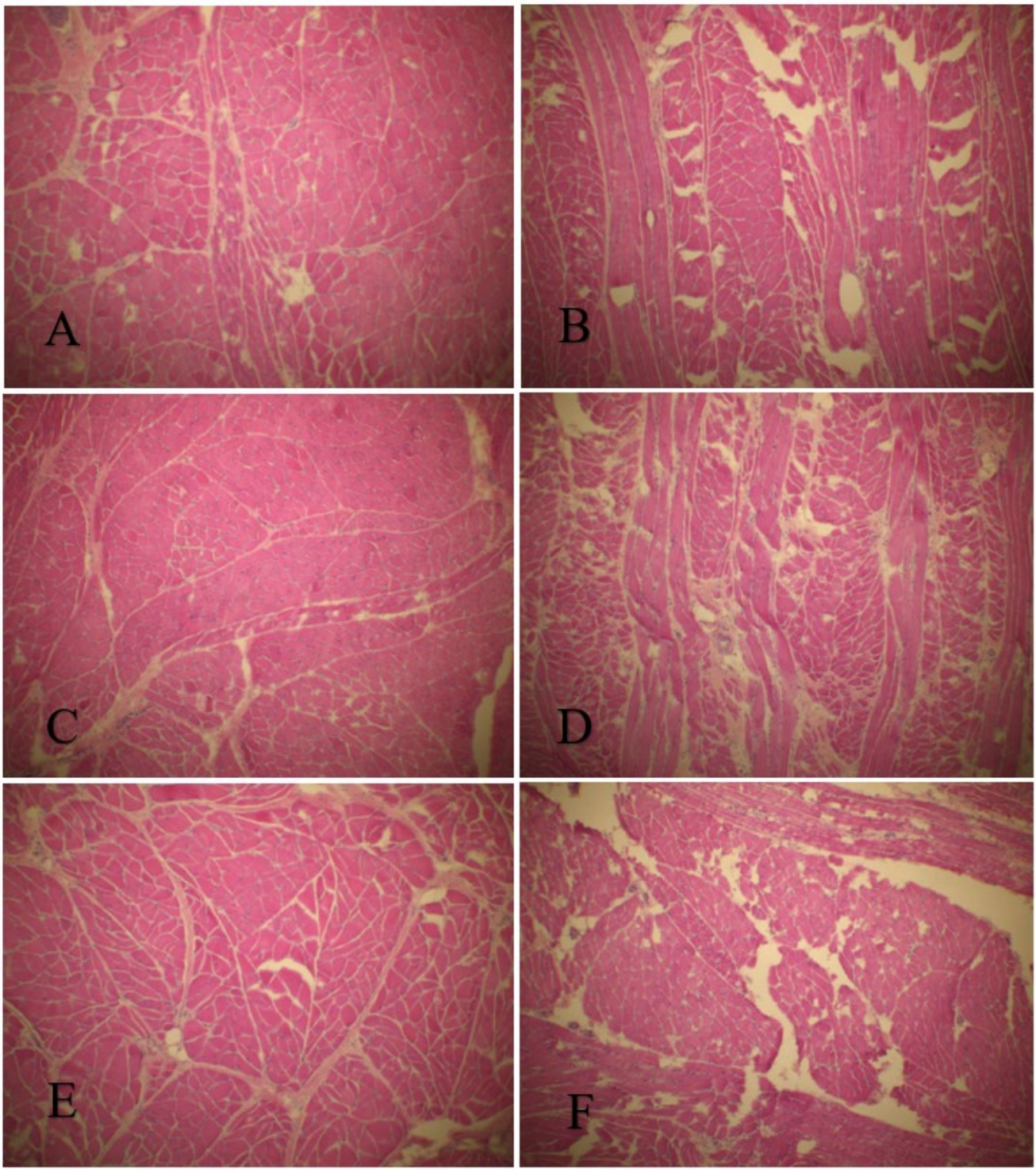

Figure 4. H&E staining of beef tongue muscle taken from **A) s**urface of the anterior region, **B)** interior of the anterior region, **C)** surface of the medial region, **D)** interior of the medial region, **E)** surface of the posterior region, and **F)** interior of the posterior region. Objective lens setting: 5x.

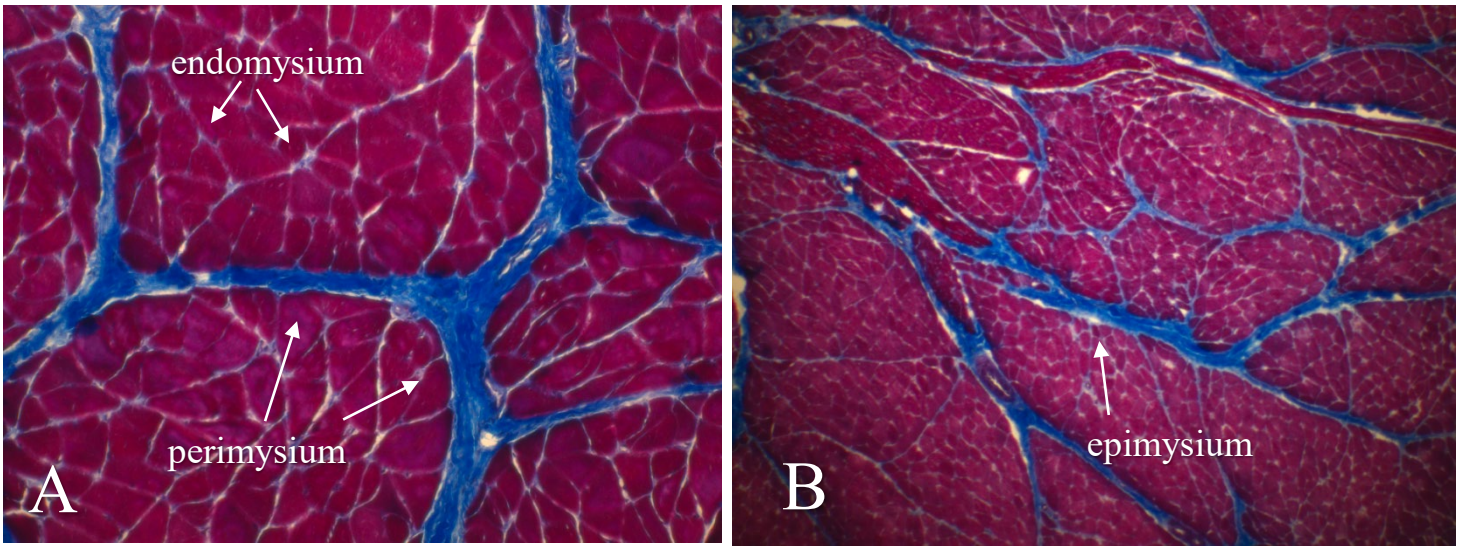

Figure 5. Masson's trichrome staining of beef tongue muscle taken from the surface of the posterior region. Objective lens setting: **A)** 10x; **B)** 5x.

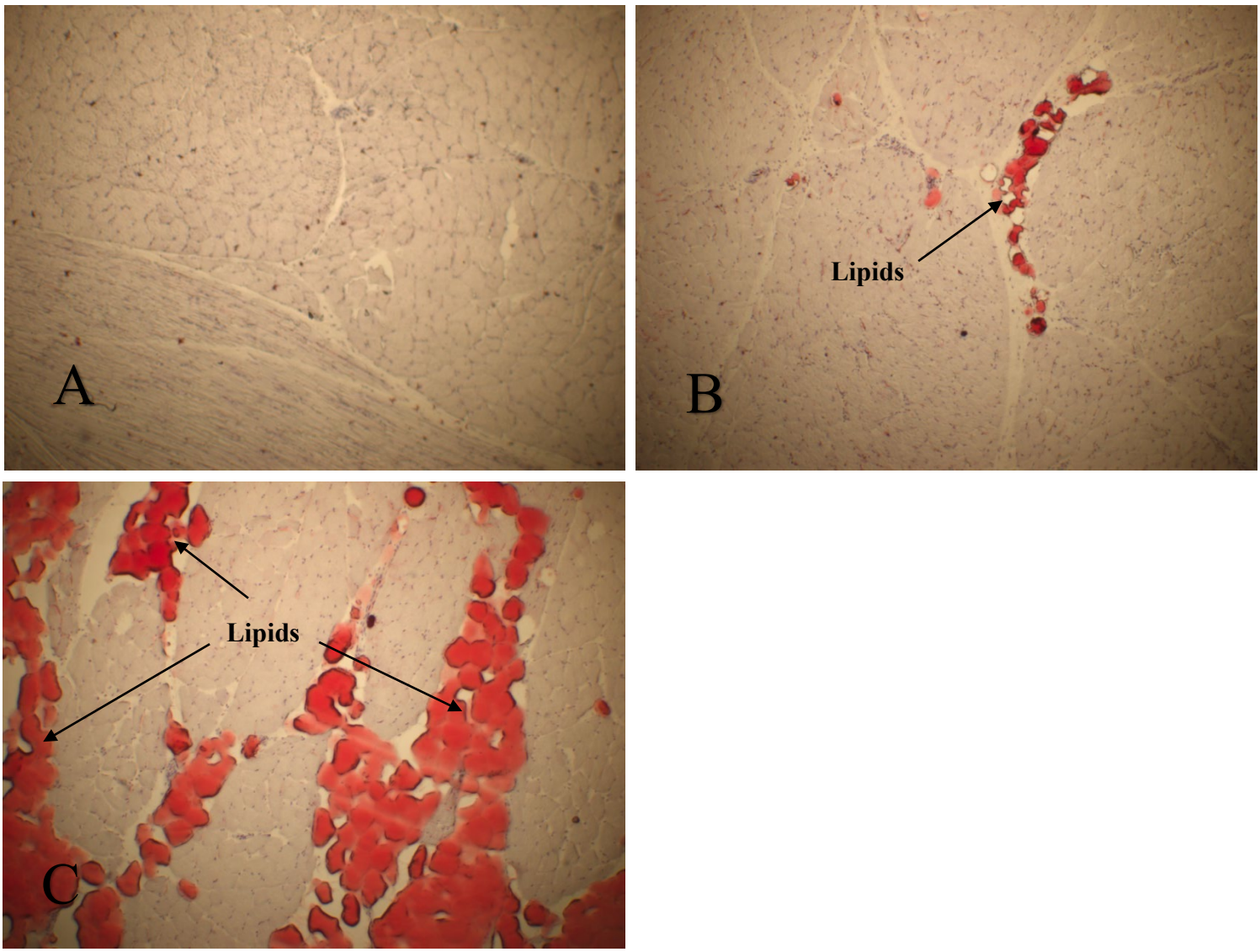

Figure 6. Oil Red O staining of beef tongue muscle taken from the **A)** anterior, **B)** medial, and **C)** posterior regions. Objective lens setting: 5x.

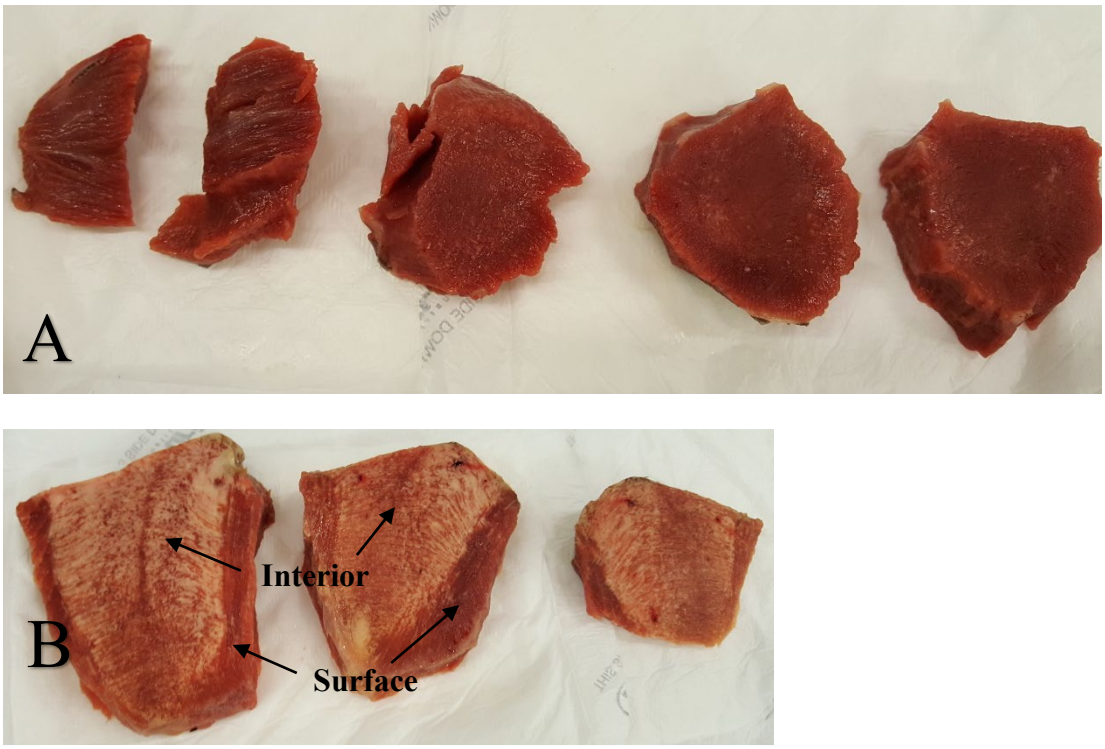

Figure 7. Dissected beef tongue muscle. **A)** anterior region, **B)** posterior region.

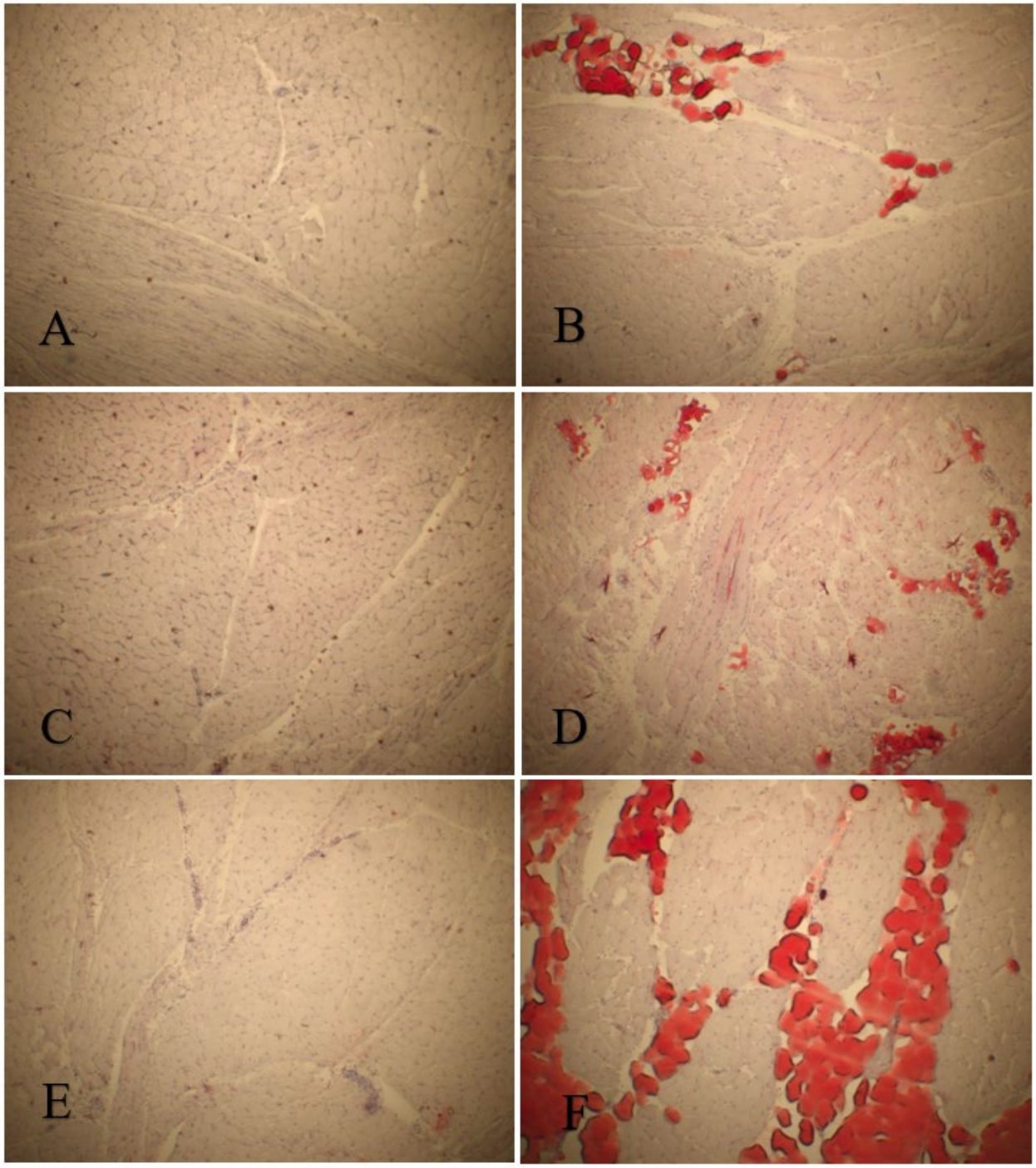

Figure 8. Oil Red O staining of beef tongue muscle taken from **A) s**urface of the anterior region, **B)** interior of the anterior region, **C)** surface of the medial region, **D)** interior of the medial region, **E)** surface of the posterior region, and **F)** interior of the posterior region. Objective lens setting: 5x.

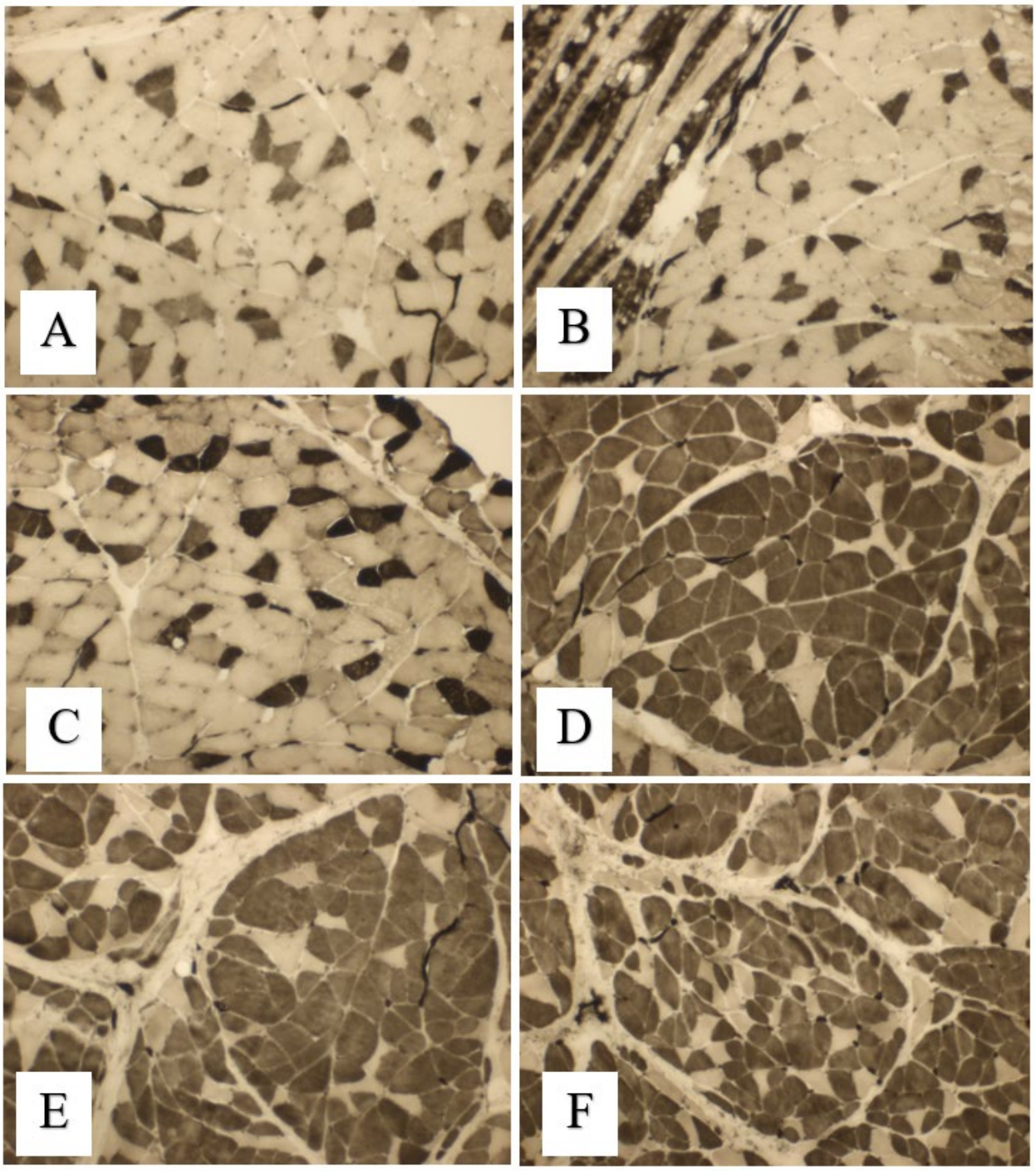

Figure 9. Fiber type staining of beef tongue taken from the surfaces muscles of the **A-C)** anterior and **D-F)** posterior regions. Dark fibers are type I (slow-twitch), and light fibers are type II (fast-twitch). Objective lens setting: 10x.

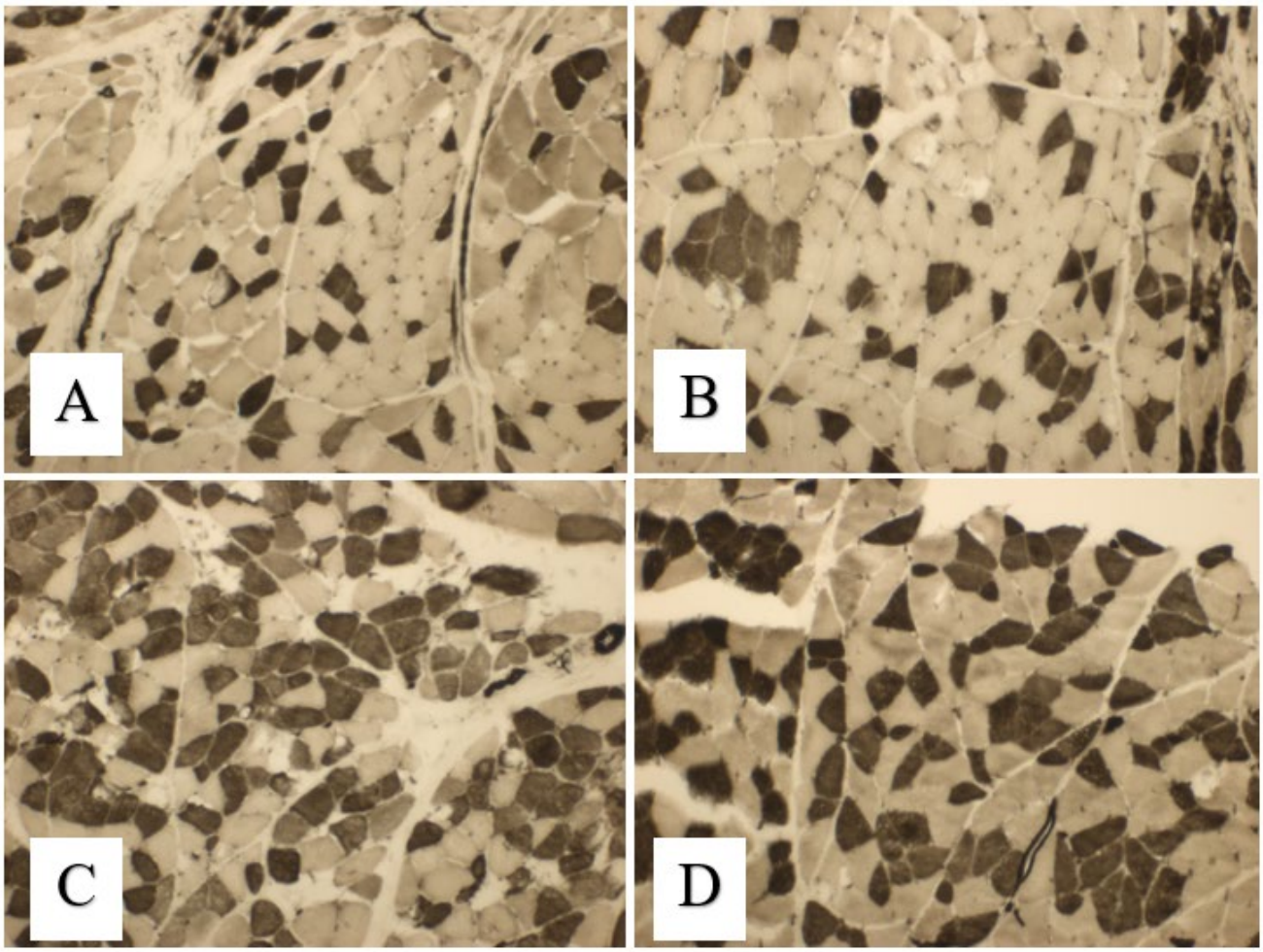

Figure 10. Fiber type staining of beef tongue taken from the **A-B)** surface and **C-D)** interior of the anterior region. Dark fibers are type I (slow-twitch), and light fibers are type II (fast-twitch). Objective lens setting: 10x.

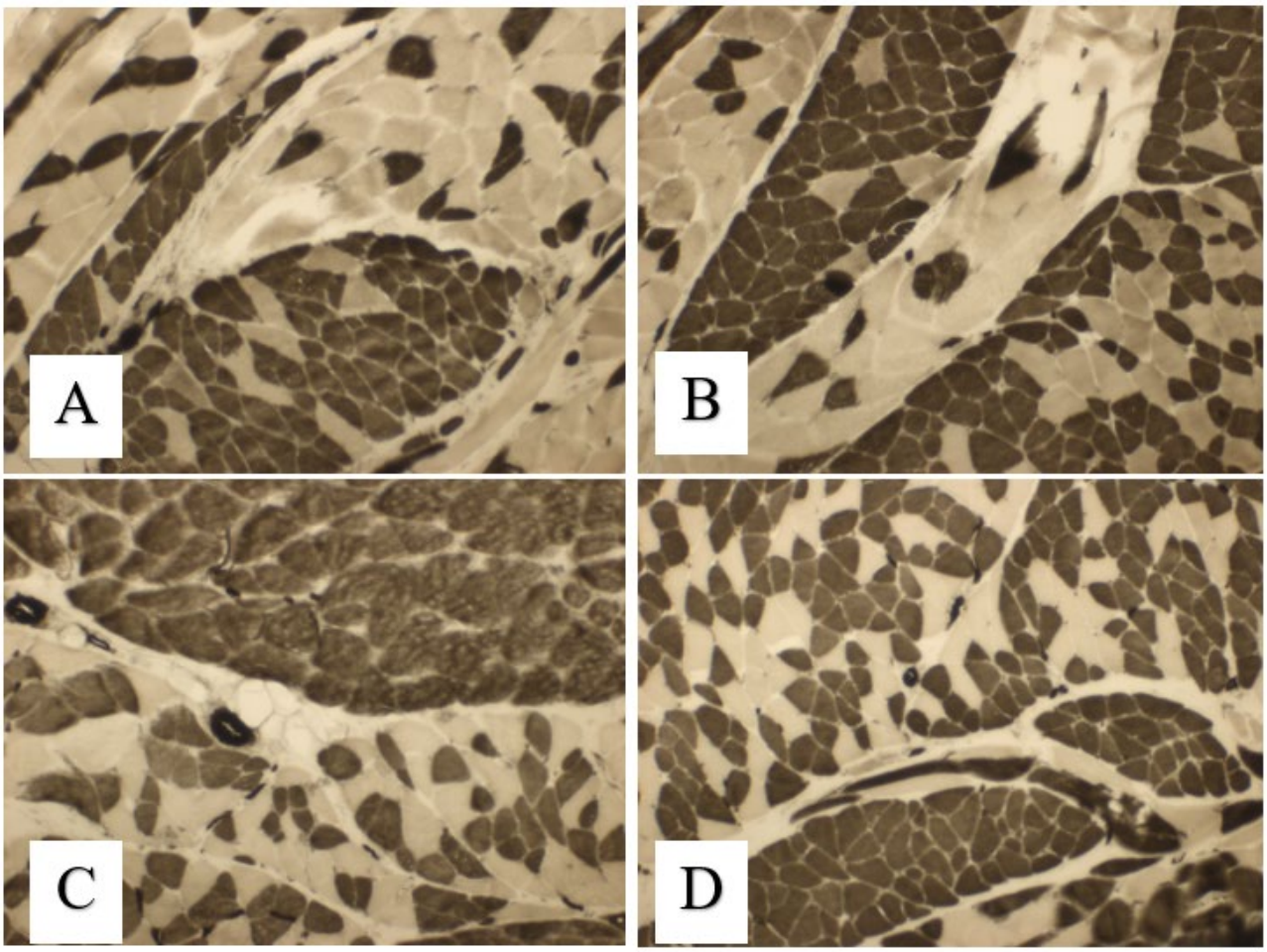

Figure 11. Fiber type staining of beef tongue. Dark fibers are type I (slow-twitch), and light fibers are type II (fast-twitch). Objective lens setting: 10x.

APPENDIX A

RELATIVE ABUNDANCE OF BEEF TONGUE SARCOPLASMIC PROTEINS

Protein	Peak Area
Myoglobin OS=Bos taurus O×=9913 GN=MB PE=1 SV=3 - [MYG_BOVIN]	3.1×10^{9}
Creatine kinase M-type OS=Bos taurus O×=9913 GN=CKM PE=1 SV=2 - [KCRM_BOVIN]	3.1×10^{9}
Glyceraldehyde-3-phosphate dehydrogenase OS=Bos taurus O×=9913 GN=GAPDH PE=1 SV=4 - [G3P_BOVIN]	3.0×10^{9}
Serum albumin OS=Bos taurus O×=9913 GN=ALB PE=1 SV=4 - [ALBU_BOVIN]	2.8×10^{9}
Actin, alpha skeletal muscle OS=Bos taurus O×=9913 GN=ACTA1 PE=1 SV=1 - [ACTS_BOVIN]	1.0×10^{9}
Hemoglobin subunit beta OS=Bos taurus O×=9913 GN=HBB PE=1 SV=1 - [HBB_BOVIN]	9.1×10^{8}
L-lactate dehydrogenase B chain OS=Bos taurus O×=9913 GN=LDHB PE=2 SV=4 - [LDHB_BOVIN]	8.0×10^{8}
L-lactate dehydrogenase A chain OS=Bos taurus O×=9913 GN=LDHA PE=2 SV=2 - [LDHA_BOVIN]	7.5×10^{8}
Hemoglobin subunit alpha OS=Bos taurus O×=9913 GN=HBA PE=1 SV=2 - [HBA_BOVIN]	7.1×10^{8}
Actin, cytoplasmic 1 OS=Bos taurus O×=9913 GN=ACTB PE=1 SV=1 - [ACTB_BOVIN]	6.3×10^{8}
Phosphoglycerate mutase 2 OS=Bos taurus O×=9913 GN=PGAM2 PE=2 SV=1 - [PGAM2_BOVIN]	6.0×10^{8}
Heat shock protein beta-1 OS=Bos taurus O×=9913 GN=HSPB1 PE=2 SV=1 - [HSPB1_BOVIN]	5.9×10^{8}
Malate dehydrogenase, cytoplasmic OS=Bos taurus O×=9913 GN=MDH1 PE=2 SV=3 - [MDHC_BOVIN]	5.7×10^{8}
Triosephosphate isomerase OS=Bos taurus O×=9913 GN=TPI1 PE=2 SV=3 - [TPIS_BOVIN]	5.7×10^{8}

Creatine kinase S-type, mitochondrial OS=Bos taurus O×=9913 GN=CKMT2 PE=2 SV=1 - [KCRS_BOVIN]	5.3×10^{8}
Myosin regulatory light chain 2, skeletal muscle isoform OS=Bos taurus O×=9913 GN=MYLPF PE=2 SV=1 - [MLRS_BOVIN]	4.7×10^{8}
Beta-enolase OS=Bos taurus O×=9913 GN=ENO3 PE=2 SV=1 - [ENOB_BOVIN]	4.7×10^{8}
Phosphatidylethanolamine-binding protein 1 OS=Bos taurus O×=9913 GN=PEBP1 PE=1 SV=2 - [PEBP1_BOVIN]	3.3×10^{8}
Glycogen phosphorylase, muscle form OS=Bos taurus O×=9913 GN=PYGM PE=1 SV=3 - [PYGM_BOVIN]	3.3×10^{8}
Malate dehydrogenase, mitochondrial OS=Bos taurus O×=9913 GN=MDH2 PE=1 SV=1 - [MDHM_BOVIN]	2.8×10^{8}
Serotransferrin OS=Bos taurus O×=9913 GN=TF PE=2 SV=1 - [TRFE_BOVIN]	2.7×10^{8}
Glutathione S-transferase P OS=Bos taurus O×=9913 GN=GSTP1 PE=1 SV=2 - [GSTP1_BOVIN]	2.3×10^{8}
Myosin light chain 1/3, skeletal muscle isoform OS=Bos taurus O×=9913 GN=MYL1 PE=2 SV=1 - [MYL1_BOVIN]	2.0×10^{8}
Phosphoglycerate kinase 1 OS=Bos taurus O×=9913 GN=PGK1 PE=2 SV=3 - [PGK1_BOVIN]	1.9×10^{8}
Aspartate aminotransferase, cytoplasmic OS=Bos taurus O×=9913 GN=GOT1 PE=1 SV=3 - [AATC_BOVIN]	1.9×10^{8}
ATP synthase subunit beta, mitochondrial OS=Bos taurus O×=9913 GN=ATP5F1B PE=1 SV=2 - [ATPB_BOVIN]	1.8×10^{8}
Alpha-enolase OS=Bos taurus O×=9913 GN=ENO1 PE=1 SV=4 - [ENOA_BOVIN]	1.6×10^{8}
Glucose-6-phosphate isomerase OS=Bos taurus O×=9913 GN=GPI PE=2 SV=4 - [G6PI_BOVIN]	1.6×10^{8}
Fructose-bisphosphate aldolase B OS=Bos taurus O×=9913 GN=ALDOB PE=2 SV=1 - [ALDOB_BOVIN]	1.4×10^{8}
Pero×iredo×in-1 OS=Bos taurus O×=9913 GN=PRD×1 PE=2 SV=1 - [PRD×1_BOVIN]	1.4×10^{8}
Heat shock 70 kDa protein 1B OS=Bos taurus O×=9913 GN=HSPA1B PE=2 SV=1 - [HS71B_BOVIN]	1.4×10^{8}
Aconitate hydratase, mitochondrial OS=Bos taurus O×=9913 GN=ACO2 PE=1 SV=4 - [ACON_BOVIN]	1.4×10^{8}

Heat shock cognate 71 kDa protein OS=Bos taurus O×=9913 GN=HSPA8 PE=1 SV=2 - [HSP7C_BOVIN]	1.4×10^{8}
Cysteine and glycine-rich protein 3 OS=Bos taurus O×=9913 GN=CSRP3 PE=2 SV=1 - [CSRP3_BOVIN]	1.3×10^{8}
Calmodulin OS=Bos taurus O×=9913 GN=CALM PE=1 SV=2 - [CALM_BOVIN]	1.3×10^{8}
Cofilin-2 OS=Bos taurus O×=9913 GN=CFL2 PE=2 SV=1 - [COF2_BOVIN]	1.2×10^{8}
Adenylate kinase isoenzyme 1 OS=Bos taurus O×=9913 GN=AK1 PE=1 SV=2 - [KAD1_BOVIN]	1.2×10^{8}
Phosphoglycerate mutase 1 OS=Bos taurus O×=9913 GN=PGAM1 PE=2 SV=3 - [PGAM1_BOVIN]	1.2×10^{8}
Supero×ide dismutase [Cu-Zn] OS=Bos taurus O×=9913 GN=SOD1 PE=1 SV=2 - [SODC_BOVIN]	1.1×10^{8}
Myosin light chain 3 OS=Bos taurus O×=9913 GN=MYL3 PE=1 SV=1 - [MYL3_BOVIN]	1.1×10^{8}
Fatty acid-binding protein, heart OS=Bos taurus O×=9913 GN=FABP3 PE=1 SV=2 - [FABPH_BOVIN]	1.0×10^{8}
Protein/nucleic acid deglycase DJ-1 OS=Bos taurus O×=9913 GN=PARK7 PE=2 SV=1 - [PARK7_BOVIN]	1.0×10^{8}
Heat shock protein beta-6 OS=Bos taurus O×=9913 GN=HSPB6 PE=2 SV=1 - [HSPB6_BOVIN]	9.9×10^{7}
Serpin A3-4 OS=Bos taurus O×=9913 GN=SERPINA3-4 PE=3 SV=1 - [SPA34_BOVIN]	9.8×10^{7}
Acyl-CoA-binding protein OS=Bos taurus O×=9913 GN=DBI PE=1 SV=2 - [ACBP_BOVIN]	9.7×10^{7}
Lumican OS=Bos taurus O×=9913 GN=LUM PE=1 SV=1 - [LUM_BOVIN]	9.3×10^{7}
Myosin regulatory light chain 2, ventricular/cardiac muscle isoform OS=Bos taurus O×=9913 GN=MYL2 PE=1 SV=1 - [MLRV_BOVIN]	9.3×10^{7}
Phosphoglucomutase-1 OS=Bos taurus O×=9913 GN=PGM1 PE=2 SV=1 - [PGM1_BOVIN]	9.1×10^{7}
Alpha-1-acid glycoprotein OS=Bos taurus O×=9913 GN=ORM1 PE=2 SV=1 - [A1AG_BOVIN]	8.7×10^{7}
Heat shock protein HSP 90-alpha OS=Bos taurus O×=9913 GN=HSP90AA1 PE=1 SV=3 - [HS90A_BOVIN]	8.2×10^{7}

Alpha-2-HS-glycoprotein OS=Bos taurus O×=9913 GN=AHSG PE=1 SV=2 - [FETUA_BOVIN]	8.1×10^{7}
Alpha-crystallin B chain OS=Bos taurus O×=9913 GN=CRYAB PE=1 SV=2 - [CRYAB_BOVIN]	8.0×10^{7}
Thioredo×in OS=Bos taurus O×=9913 GN=T×N PE=3 SV=3 - [THIO_BOVIN]	8.0×10^{7}
Aspartate aminotransferase, mitochondrial OS=Bos taurus O×=9913 GN=GOT2 PE=1 SV=2 - [AATM_BOVIN]	8.0×10^{7}
Serpin A3-2 OS=Bos taurus O×=9913 GN=SERPINA3-2 PE=3 SV=1 - [SPA32_BOVIN]	7.8×10^{7}
Pero×iredo×in-2 OS=Bos taurus O×=9913 GN=PRD×2 PE=2 SV=1 - [PRD×2_BOVIN]	7.5×10^{7}
Citrate synthase, mitochondrial OS=Bos taurus O×=9913 GN=CS PE=1 SV=1 - [CISY_BOVIN]	7.4×10^{7}
PDZ and LIM domain protein 3 OS=Bos taurus O×=9913 GN=PDLIM3 PE=2 SV=1 - [PDLI3_BOVIN]	7.3×10^{7}
Retinal dehydrogenase 1 OS=Bos taurus O×=9913 GN=ALDH1A1 PE=1 SV=3 - [AL1A1_BOVIN]	6.8×10^{7}
Hemope×in OS=Bos taurus O×=9913 GN=HP× PE=2 SV=1 - [HEMO_BOVIN]	6.8×10^{7}
Alpha-1B-glycoprotein OS=Bos taurus O×=9913 GN=A1BG PE=1 SV=1 - [A1BG_BOVIN]	6.7×10^{7}
Heat shock protein HSP 90-beta OS=Bos taurus O×=9913 GN=HSP90AB1 PE=2 SV=3 - [HS90B_BOVIN]	6.7×10^{7}
Flavin reductase (NADPH) OS=Bos taurus O×=9913 GN=BLVRB PE=1 SV=2 - [BLVRB_BOVIN]	6.6×10^{7}
Elongation factor 1-alpha 2 OS=Bos taurus O×=9913 GN=EEF1A2 PE=2 SV=1 - [EF1A2_BOVIN]	6.4×10^{7}
Glutathione S-transferase Mu 1 OS=Bos taurus O×=9913 GN=GSTM1 PE=1 SV=3 - [GSTM1_BOVIN]	6.3×10^{7}
Apolipoprotein A-I OS=Bos taurus O×=9913 GN=APOA1 PE=1 SV=3 - [APOA1_BOVIN]	6.2×10^{7}
Tropomyosin beta chain OS=Bos taurus O×=9913 GN=TPM2 PE=2 SV=1 - [TPM2_BOVIN]	5.6×10^{7}
Vimentin OS=Bos taurus O×=9913 GN=VIM PE=1 SV=3 - [VIME_BOVIN]	5.5×10^{7}

Galectin-1 OS=Bos taurus O×=9913 GN=LGALS1 PE=1 SV=2 - [LEG1_BOVIN]	5.5×10^{7}
Isocitrate dehydrogenase [NADP], mitochondrial OS=Bos taurus O×=9913 GN=IDH2 PE=1 SV=2 - [IDHP_BOVIN]	5.4×10^{7}
ATP-dependent 6-phosphofructokinase, muscle type OS=Bos taurus O×=9913 GN=PFKM PE=2 SV=1 - [PFKAM_BOVIN]	5.2×10^{7}
Cytochrome c OS=Bos taurus O×=9913 GN=CYCS PE=1 SV=2 - [CYC_BOVIN]	5.0×10^{7}
Tropomyosin alpha-1 chain OS=Bos taurus O×=9913 GN=TPM1 PE=2 SV=1 - [TPM1_BOVIN]	5.0×10^{7}
14-3-3 protein gamma OS=Bos taurus O×=9913 GN=YWHAG PE=1 SV=2 - [1433G_BOVIN]	4.9×10^{7}
Anne×in A2 OS=Bos taurus O×=9913 GN=AN×A2 PE=1 SV=2 - [AN×A2_BOVIN]	4.8×10^{7}
Alpha-1-antiproteinase OS=Bos taurus O×=9913 GN=SERPINA1 PE=1 SV=1 - [A1AT_BOVIN]	4.8×10^{7}
Tropomyosin alpha-3 chain OS=Bos taurus O×=9913 GN=TPM3 PE=2 SV=1 - [TPM3_BOVIN]	4.7×10^{7}
ADP-ribose glycohydrolase MACROD1 OS=Bos taurus O×=9913 GN=MACROD1 PE=2 SV=1 - [MACD1_BOVIN]	4.6×10^{7}
Fatty acid-binding protein, adipocyte OS=Bos taurus O×=9913 GN=FABP4 PE=2 SV=2 - [FABP4_BOVIN]	4.5×10^{7}
14-3-3 protein epsilon OS=Bos taurus O×=9913 GN=YWHAE PE=2 SV=1 - [1433E_BOVIN]	4.4×10^{7}
Troponin C, slow skeletal and cardiac muscles OS=Bos taurus O×=9913 GN=TNNC1 PE=1 SV=1 - [TNNC1_BOVIN]	4.3×10^{7}
Endoplasmic reticulum chaperone BiP OS=Bos taurus O×=9913 GN=HSPA5 PE=2 SV=1 - [BIP_BOVIN]	4.2×10^{7}
14 kDa phosphohistidine phosphatase OS=Bos taurus O×=9913 GN=PHPT1 PE=2 SV=1 - [PHP14_BOVIN]	4.1×10^{7}
Kininogen-2 OS=Bos taurus O×=9913 GN=KNG2 PE=1 SV=1 - [KNG2_BOVIN]	4.0×10^{7}
Kininogen-1 OS=Bos taurus O×=9913 GN=KNG1 PE=1 SV=1 - [KNG1_BOVIN]	4.0×10^{7}

Transthyretin OS=Bos taurus O×=9913 GN=TTR PE=1 SV=1 - [TTHY_BOVIN]	4.0×10^{7}
Anne×in A5 OS=Bos taurus O×=9913 GN=AN×A5 PE=1 SV=3 - [AN×A5_BOVIN]	3.9×10^{7}
Protein NDRG2 OS=Bos taurus O×=9913 GN=NDRG2 PE=2 SV=1 - [NDRG2_BOVIN]	3.7×10^{7}
Serpin A3-7 OS=Bos taurus O×=9913 GN=SERPINA3-7 PE=3 SV=1 - [SPA37_BOVIN]	3.6×10^{7}
Profilin-1 OS=Bos taurus O×=9913 GN=PFN1 PE=1 SV=2 - [PROF1_BOVIN]	3.5×10^{7}
Anne×in A6 OS=Bos taurus O×=9913 GN=AN×A6 PE=1 SV=2 - [AN×A6_BOVIN]	3.5×10^{7}
Protein HP-20 homolog OS=Bos taurus O×=9913 PE=2 SV=1 - [HP20_BOVIN]	3.5×10^{7}
Mth938 domain-containing protein OS=Bos taurus O×=9913 GN=AAMDC PE=2 SV=1 - [AAMDC_BOVIN]	3.5×10^{7}
Nucleoside diphosphate kinase B OS=Bos taurus O×=9913 GN=NME2 PE=1 SV=1 - [NDKB_BOVIN]	3.4×10^{7}
Glycerol-3-phosphate dehydrogenase [NAD(+)], cytoplasmic OS=Bos taurus O×=9913 GN=GPD1 PE=2 SV=3 - [GPDA_BOVIN]	3.4×10^{7}
Four and a half LIM domains protein 3 OS=Bos taurus O×=9913 GN=FHL3 PE=2 SV=1 - [FHL3_BOVIN]	3.4×10^{7}
Transgelin OS=Bos taurus O×=9913 GN=TAGLN PE=1 SV=4 - [TAGL_BOVIN]	3.4×10^{7}
Alpha-aminoadipic semialdehyde dehydrogenase OS=Bos taurus O×=9913 GN=ALDH7A1 PE=2 SV=4 - [AL7A1_BOVIN]	3.4×10^{7}
Peptidyl-prolyl cis-trans isomerase A OS=Bos taurus O×=9913 GN=PPIA PE=1 SV=2 - [PPIA_BOVIN]	3.2×10^{7}
Serine/threonine-protein phosphatase 2A 65 kDa regulatory subunit A alpha isoform OS=Bos taurus O×=9913 GN=PPP2R1A PE=1 SV=1 - [2AAA_BOVIN]	3.2×10^{7}
UTP--glucose-1-phosphate uridylyltransferase OS=Bos taurus O×=9913 GN=UGP2 PE=1 SV=2 - [UGPA_BOVIN]	3.2×10^{7}
Pero×iredo×in-6 OS=Bos taurus O×=9913 GN=PRD×6 PE=1 SV=3 - [PRD×6_BOVIN]	3.2×10^{7}
Histidine triad nucleotide-binding protein 1 OS=Bos taurus O×=9913 GN=HINT1 PE=1 SV=2 - [HINT1_BOVIN]	3.2×10^{7}

14-3-3 protein beta/alpha OS=Bos taurus O×=9913 GN=YWHAB PE=1 SV=2 - [1433B_BOVIN]	3.0×10^{7}
Musculoskeletal embryonic nuclear protein 1 OS=Bos taurus O×=9913 GN=MUSTN1 PE=3 SV=1 - [MSTN1_BOVIN]	2.9×10^{7}
14-3-3 protein zeta/delta OS=Bos taurus O×=9913 GN=YWHAZ PE=1 SV=1 - [1433Z_BOVIN]	2.9×10^{7}
Alpha-actinin-2 OS=Bos taurus O×=9913 GN=ACTN2 PE=2 SV=1 - [ACTN2_BOVIN]	2.9×10^{7}
Protein HP-25 homolog 2 OS=Bos taurus O×=9913 PE=2 SV=1 - [HP252_BOVIN]	2.9×10^{7}
Anne×in A3 OS=Bos taurus O×=9913 GN=AN×A3 PE=2 SV=3 - [AN×A3_BOVIN]	2.8×10^{7}
14-3-3 protein eta OS=Bos taurus O×=9913 GN=YWHAH PE=1 SV=2 - [1433F_BOVIN]	2.7×10^{7}
Alpha-2-macroglobulin OS=Bos taurus O×=9913 GN=A2M PE=1 SV=2 - [A2MG_BOVIN]	2.7×10^{7}
Fatty acid-binding protein 5 OS=Bos taurus O×=9913 GN=FABP5 PE=1 SV=4 - [FABP5_BOVIN]	2.7×10^{7}
Vitamin D-binding protein OS=Bos taurus O×=9913 GN=GC PE=2 SV=1 - [VTDB_BOVIN]	2.7×10^{7}
Acetyl-CoA acetyltransferase, mitochondrial OS=Bos taurus O×=9913 GN=ACAT1 PE=2 SV=1 - [THIL_BOVIN]	2.7×10^{7}
Complement C3 OS=Bos taurus O×=9913 GN=C3 PE=1 SV=2 - [CO3_BOVIN]	2.7×10^{7}
LIM and cysteine-rich domains protein 1 OS=Bos taurus O×=9913 GN=LMCD1 PE=2 SV=1 - [LMCD1_BOVIN]	2.6×10^{7}
Protein S100-A4 OS=Bos taurus O×=9913 GN=S100A4 PE=1 SV=2 - [S10A4_BOVIN]	2.6×10^{7}
Small muscular protein OS=Bos taurus O×=9913 GN=SMP× PE=3 SV=1 - [SMP×_BOVIN]	2.6×10^{7}
Macrophage migration inhibitory factor OS=Bos taurus O×=9913 GN=MIF PE=1 SV=6 - [MIF_BOVIN]	2.4×10^{7}
Zeta-crystallin OS=Bos taurus O×=9913 GN=CRYZ PE=2 SV=2 - [QOR_BOVIN]	2.4×10^{7}
Purine nucleoside phosphorylase OS=Bos taurus O×=9913 GN=PNP PE=1 SV=3 - [PNPH_BOVIN]	2.4×10^{7}

Acylphosphatase-2 OS=Bos taurus O×=9913 GN=ACYP2 PE=1 SV=2 - [ACYP2_BOVIN]	2.4×10^{7}
Eukaryotic translation initiation factor 5A-1 OS=Bos taurus O×=9913 GN=EIF5A PE=2 SV=3 - [IF5A1_BOVIN]	2.4×10^{7}
Stress-induced-phosphoprotein 1 OS=Bos taurus O×=9913 GN=STIP1 PE=2 SV=1 - [STIP1_BOVIN]	2.4×10^{7}
Myosin light polypeptide 6 OS=Bos taurus O×=9913 GN=MYL6 PE=2 SV=2 - [MYL6_BOVIN]	2.3×10^{7}
Electron transfer flavoprotein subunit alpha, mitochondrial OS=Bos taurus O×=9913 GN=ETFA PE=2 SV=1 - [ETFA_BOVIN]	2.3×10^{7}
Ubiquitin carbo×yl-terminal hydrolase isozyme L1 OS=Bos taurus O×=9913 GN=UCHL1 PE=1 SV=2 - [UCHL1_BOVIN]	2.3×10^{7}
Medium-chain specific acyl-CoA dehydrogenase, mitochondrial OS=Bos taurus O×=9913 GN=ACADM PE=2 SV=1 - [ACADM_BOVIN]	2.2×10^{7}
10 kDa heat shock protein, mitochondrial OS=Bos taurus O×=9913 GN=HSPE1 PE=3 SV=2 - [CH10_BOVIN]	2.2×10^{7}
Protein HP-25 homolog 1 OS=Bos taurus O×=9913 PE=1 SV=1 - [HP251_BOVIN]	2.2×10^{7}
Electron transfer flavoprotein subunit beta OS=Bos taurus O×=9913 GN=ETFB PE=1 SV=3 - [ETFB_BOVIN]	2.1×10^{7}
Pyruvate dehydrogenase E1 component subunit beta, mitochondrial OS=Bos taurus O×=9913 GN=PDHB PE=1 SV=2 - [ODPB_BOVIN]	2.1×10^{7}
Alcohol dehydrogenase class-3 OS=Bos taurus O×=9913 GN=ADH5 PE=2 SV=1 - [ADH×_BOVIN]	2.1×10^{7}
ATPase inhibitor, mitochondrial OS=Bos taurus O×=9913 GN=ATP5IF1 PE=1 SV=2 - [ATIF1_BOVIN]	2.1×10^{7}
Decorin OS=Bos taurus O×=9913 GN=DCN PE=1 SV=2 - [PGS2_BOVIN]	2.1×10^{7}
Anne×in A1 OS=Bos taurus O×=9913 GN=AN×A1 PE=1 SV=2 - [AN×A1_BOVIN]	2.0×10^{7}
Mitochondrial peptide methionine sulfo×ide reductase OS=Bos taurus O×=9913 GN=MSRA PE=1 SV=2 - [MSRA_BOVIN]	2.0×10^{7}
Adenosylhomocysteinase OS=Bos taurus O×=9913 GN=AHCY PE=2 SV=3 - [SAHH_BOVIN]	2.0×10^{7}
ATP synthase subunit alpha, mitochondrial OS=Bos taurus O×=9913 GN=ATP5F1A PE=1 SV=1 - [ATPA_BOVIN]	1.9×10^{7}

ATP synthase subunit delta, mitochondrial OS=Bos taurus O×=9913 GN=ATP5F1D PE=1 SV=2 - [ATPD_BOVIN]	1.8×10^{7}
Elongation factor 2 OS=Bos taurus O×=9913 GN=EEF2 PE=2 SV=3 - [EF2_BOVIN]	1.8×10^{7}
Adiponectin OS=Bos taurus O×=9913 GN=ADIPOQ PE=1 SV=1 - [ADIPO_BOVIN]	1.8×10^{7}
Desmin OS=Bos taurus O×=9913 GN=DES PE=2 SV=3 - [DESM_BOVIN]	1.8×10^{7}
S-formylglutathione hydrolase OS=Bos taurus O×=9913 GN=ESD PE=2 SV=1 - [ESTD_BOVIN]	1.8×10^{7}
Fructose-1,6-bisphosphatase isozyme 2 OS=Bos taurus O×=9913 GN=FBP2 PE=2 SV=1 - [F16P2_BOVIN]	1.7×10^{7}
Eukaryotic initiation factor 4A-II OS=Bos taurus O×=9913 GN=EIF4A2 PE=2 SV=1 - [IF4A2_BOVIN]	1.7×10^{7}
Thioredo×in-dependent pero×ide reductase, mitochondrial OS=Bos taurus O×=9913 GN=PRD×3 PE=1 SV=2 - [PRD×3_BOVIN]	1.6×10^{7}
Pyruvate dehydrogenase E1 component subunit alpha, somatic form, mitochondrial OS=Bos taurus O×=9913 GN=PDHA1 PE=2 SV=1 - [ODPA_BOVIN]	1.6×10^{7}
3-ketoacyl-CoA thiolase, mitochondrial OS=Bos taurus O×=9913 GN=ACAA2 PE=2 SV=1 - [THIM_BOVIN]	1.6×10^{7}
Nuclear transport factor 2 OS=Bos taurus O×=9913 GN=NUTF2 PE=2 SV=1 - [NTF2_BOVIN]	1.6×10^{7}
Stress-70 protein, mitochondrial OS=Bos taurus O×=9913 GN=HSPA9 PE=2 SV=1 - [GRP75_BOVIN]	1.5×10^{7}
Succinate--CoA ligase [GDP-forming] subunit beta, mitochondrial OS=Bos taurus O×=9913 GN=SUCLG2 PE=2 SV=1 - [SUCB2_BOVIN]	1.5×10^{7}
ADP/ATP translocase 1 OS=Bos taurus O×=9913 GN=SLC25A4 PE=1 SV=3 - [ADT1_BOVIN]	1.5×10^{7}
Very long-chain specific acyl-CoA dehydrogenase, mitochondrial OS=Bos taurus O×=9913 GN=ACADVL PE=2 SV=3 - [ACADV_BOVIN]	1.5×10^{7}
Aldo-keto reductase family 1 member A1 OS=Bos taurus O×=9913 GN=AKR1A1 PE=2 SV=1 - [AK1A1_BOVIN]	1.4×10^{7}
Ubiquitin carbo×yl-terminal hydrolase isozyme L3 OS=Bos taurus O×=9913 GN=UCHL3 PE=2 SV=1 - [UCHL3_BOVIN]	1.4×10^{7}

Ubiquitin-like modifier-activating enzyme 1 OS=Bos taurus O×=9913 GN=UBA1 PE=2 SV=1 - [UBA1_BOVIN]	1.4×10^{7}
Glycogen [starch] synthase, muscle OS=Bos taurus O×=9913 GN=GYS1 PE=2 SV=1 - [GYS1_BOVIN]	1.4×10^{7}
Sarcoplasmic/endoplasmic reticulum calcium ATPase 1 OS=Bos taurus O×=9913 GN=ATP2A1 PE=1 SV=1 - [AT2A1_BOVIN]	1.4×10^{7}
Poly(rC)-binding protein 1 OS=Bos taurus O×=9913 GN=PCBP1 PE=2 SV=1 - [PCBP1_BOVIN]	1.4×10^{7}
Alpha-actinin-4 OS=Bos taurus O×=9913 GN=ACTN4 PE=2 SV=1 - [ACTN4_BOVIN]	1.3×10^{7}
Aldo-keto reductase family 1 member B1 OS=Bos taurus O×=9913 GN=AKR1B1 PE=1 SV=2 - [ALDR_BOVIN]	1.3×10^{7}
Rho GDP-dissociation inhibitor 1 OS=Bos taurus O×=9913 GN=ARHGDIA PE=1 SV=3 - [GDIR1_BOVIN]	1.3×10^{7}
Protein-L-isoaspartate(D-aspartate) O-methyltransferase OS=Bos taurus O×=9913 GN=PCMT1 PE=1 SV=2 - [PIMT_BOVIN]	1.3×10^{7}
Electrogenic sodium bicarbonate cotransporter 1 OS=Bos taurus O×=9913 GN=SLC4A4 PE=1 SV=1 - [S4A4_BOVIN]	1.3×10^{7}
Short-chain specific acyl-CoA dehydrogenase, mitochondrial OS=Bos taurus O×=9913 GN=ACADS PE=1 SV=1 - [ACADS_BOVIN]	1.3×10^{7}
Elongation factor 1-delta OS=Bos taurus O×=9913 GN=EEF1D PE=2 SV=2 - [EF1D_BOVIN]	1.2×10^{7}
Fibrinogen gamma-B chain OS=Bos taurus O×=9913 GN=FGG PE=1 SV=1 - [FIBG_BOVIN]	1.2×10^{7}
Transitional endoplasmic reticulum ATPase OS=Bos taurus O×=9913 GN=VCP PE=2 SV=1 - [TERA_BOVIN]	1.2×10^{7}
Calpain small subunit 1 OS=Bos taurus O×=9913 GN=CAPNS1 PE=2 SV=1 - [CPNS1_BOVIN]	1.1×10^{7}
Complement factor B OS=Bos taurus O×=9913 GN=CFB PE=1 SV=2 - [CFAB_BOVIN]	1.1×10^{7}
60 kDa heat shock protein, mitochondrial OS=Bos taurus O×=9913 GN=HSPD1 PE=1 SV=2 - [CH60_BOVIN]	1.1×10^{7}
Adenylate kinase 2, mitochondrial OS=Bos taurus O×=9913 GN=AK2 PE=1 SV=2 - [KAD2_BOVIN]	1.1×10^{7}

GTP:AMP phosphotransferase AK3, mitochondrial OS=Bos taurus O×=9913 GN=AK3 PE=1 SV=3 - [KAD3_BOVIN]	1.1×10^{7}
Mimecan OS=Bos taurus O×=9913 GN=OGN PE=1 SV=2 - [MIME_BOVIN]	1.1×10^{7}
Enoyl-CoA hydratase, mitochondrial OS=Bos taurus O×=9913 GN=ECHS1 PE=2 SV=1 - [ECHM_BOVIN]	1.1×10^{7}
Peptidyl-prolyl cis-trans isomerase FKBP3 OS=Bos taurus O×=9913 GN=FKBP3 PE=1 SV=2 - [FKBP3_BOVIN]	1.1×10^{7}
Adenylosuccinate synthetase isozyme 1 OS=Bos taurus O×=9913 GN=ADSSL1 PE=2 SV=1 - [PURA1_BOVIN]	1.0×10^{7}
Asparagine--tRNA ligase, cytoplasmic OS=Bos taurus O×=9913 GN=NARS PE=2 SV=3 - [SYNC_BOVIN]	1.0×10^{7}
Dihydrolipoyllysine-residue succinyltransferase component of 2-o×oglutarate dehydrogenase comple×, mitochondrial OS=Bos taurus O×=9913 GN=DLST PE=1 SV=2 - [ODO2_BOVIN]	1.0×10^{7}
Anne×in A7 OS=Bos taurus O×=9913 GN=AN×A7 PE=1 SV=2 - [AN×A7_BOVIN]	1.0×10^{7}
Gelsolin OS=Bos taurus O×=9913 GN=GSN PE=2 SV=1 - [GELS_BOVIN]	1.0×10^{7}
Rab GDP dissociation inhibitor beta OS=Bos taurus O×=9913 GN=GDI2 PE=2 SV=3 - [GDIB_BOVIN]	9.8×10^{6}
Obg-like ATPase 1 OS=Bos taurus O×=9913 GN=OLA1 PE=2 SV=1 - [OLA1_BOVIN]	9.7×10^{6}
Cadherin-13 OS=Bos taurus O×=9913 GN=CDH13 PE=2 SV=1 - [CAD13_BOVIN]	9.7×10^{6}
cAMP-dependent protein kinase type I-alpha regulatory subunit OS=Bos taurus O×=9913 GN=PRKAR1A PE=1 SV=2 - [KAP0_BOVIN]	9.6×10^{6}
Protein disulfide-isomerase A3 OS=Bos taurus O×=9913 GN=PDIA3 PE=2 SV=1 - [PDIA3_BOVIN]	9.6×10^{6}
Proteasome subunit beta type-6 OS=Bos taurus O×=9913 GN=PSMB6 PE=1 SV=1 - [PSB6_BOVIN]	9.6×10^{6}
Tubulin polymerization-promoting protein family member 3 OS=Bos taurus O×=9913 GN=TPPP3 PE=1 SV=1 - [TPPP3_BOVIN]	9.5×10^{6}
Ubiquitin-conjugating enzyme E2 variant 2 OS=Bos taurus O×=9913 GN=UBE2V2 PE=2 SV=3 - [UB2V2_BOVIN]	9.4×10^{6}
Isovaleryl-CoA dehydrogenase, mitochondrial OS=Bos taurus O×=9913 GN=IVD PE=2 SV=1 - [IVD_BOVIN]	9.4×10^{6}

Fibrinogen beta chain OS=Bos taurus O×=9913 GN=FGB PE=1 SV=2 - [FIBB_BOVIN]	9.3×10^{6}
Apolipoprotein A-IV OS=Bos taurus O×=9913 GN=APOA4 PE=2 SV=1 - [APOA4_BOVIN]	9.3×10^{6}
Aldehyde dehydrogenase, mitochondrial OS=Bos taurus O×=9913 GN=ALDH2 PE=1 SV=2 - [ALDH2_BOVIN]	9.1×10^{6}
Fibrinogen alpha chain OS=Bos taurus O×=9913 GN=FGA PE=1 SV=5 - [FIBA_BOVIN]	9.1×10^{6}
Bifunctional purine biosynthesis protein PURH OS=Bos taurus O×=9913 GN=ATIC PE=2 SV=1 - [PUR9_BOVIN]	9.1×10^{6}
Fibrillin-1 OS=Bos taurus O×=9913 GN=FBN1 PE=1 SV=2 - [FBN1_BOVIN]	9.0×10^{6}
Ubiquinone biosynthesis protein COQ9, mitochondrial OS=Bos taurus O×=9913 GN=COQ9 PE=2 SV=1 - [COQ9_BOVIN]	8.9×10^{6}
Apolipoprotein A-II OS=Bos taurus O×=9913 GN=APOA2 PE=1 SV=2 - [APOA2_BOVIN]	8.8×10^{6}
Myosin-7 OS=Bos taurus O×=9913 GN=MYH7 PE=1 SV=1 - [MYH7_BOVIN]	8.6×10^{6}
Prolargin OS=Bos taurus O×=9913 GN=PRELP PE=2 SV=1 - [PRELP_BOVIN]	8.5×10^{6}
Tropomodulin-4 OS=Bos taurus O×=9913 GN=TMOD4 PE=2 SV=1 - [TMOD4_BOVIN]	8.2×10^{6}
Alpha-2-antiplasmin OS=Bos taurus O×=9913 GN=SERPINF2 PE=1 SV=2 - [A2AP_BOVIN]	8.2×10^{6}
Prothrombin OS=Bos taurus O×=9913 GN=F2 PE=1 SV=2 - [THRB_BOVIN]	8.0×10^{6}
NSFL1 cofactor p47 OS=Bos taurus O×=9913 GN=NSFL1C PE=2 SV=1 - [NSF1C_BOVIN]	7.9×10^{6}
Cytosol aminopeptidase OS=Bos taurus O×=9913 GN=LAP3 PE=1 SV=3 - [AMPL_BOVIN]	7.8×10^{6}
Moesin OS=Bos taurus O×=9913 GN=MSN PE=2 SV=3 - [MOES_BOVIN]	7.5×10^{6}
Prostaglandin reductase 2 OS=Bos taurus O×=9913 GN=PTGR2 PE=2 SV=1 - [PTGR2_BOVIN]	7.4×10^{6}
Cathepsin D OS=Bos taurus O×=9913 GN=CTSD PE=1 SV=2 - [CATD_BOVIN]	7.3×10^{6}
WD repeat-containing protein 1 OS=Bos taurus O×=9913 GN=WDR1 PE=2 SV=3 - [WDR1_BOVIN]	7.3×10^{6}

Metallothionein-1 OS=Bos taurus O×=9913 GN=MT1 PE=1 SV=1 - [MT1_BOVIN]	7.2×10^{6}
Transgelin-2 OS=Bos taurus O×=9913 GN=TAGLN2 PE=2 SV=3 - [TAGL2_BOVIN]	7.1×10^{6}
Myosin-2 OS=Bos taurus O×=9913 GN=MYH2 PE=2 SV=1 - [MYH2_BOVIN]	7.1×10^{6}
Histidine triad nucleotide-binding protein 2, mitochondrial OS=Bos taurus O×=9913 GN=HINT2 PE=2 SV=1 - [HINT2_BOVIN]	7.1×10^{6}
cAMP-dependent protein kinase catalytic subunit alpha OS=Bos taurus O×=9913 GN=PRKACA PE=1 SV=3 - [KAPCA_BOVIN]	7.1×10^{6}
GTP-binding protein SAR1b OS=Bos taurus O×=9913 GN=SAR1B PE=2 SV=1 - [SAR1B_BOVIN]	7.0×10^{6}
PDZ and LIM domain protein 1 OS=Bos taurus O×=9913 GN=PDLIM1 PE=2 SV=3 - [PDLI1_BOVIN]	6.7×10^{6}
Tubulin beta-5 chain OS=Bos taurus O×=9913 GN=TUBB5 PE=2 SV=1 - [TBB5_BOVIN]	6.6×10^{6}
Calpain-2 catalytic subunit OS=Bos taurus O×=9913 GN=CAPN2 PE=2 SV=2 - [CAN2_BOVIN]	6.6×10^{6}
Succinate--CoA ligase [ADP-forming] subunit beta, mitochondrial OS=Bos taurus O×=9913 GN=SUCLA2 PE=2 SV=1 - [SUCB1_BOVIN]	6.5×10^{6}
Adenylosuccinate lyase OS=Bos taurus O×=9913 GN=ADSL PE=2 SV=1 - [PUR8_BOVIN]	6.3×10^{6}
Tubulin alpha-4A chain OS=Bos taurus O×=9913 GN=TUBA4A PE=1 SV=2 - [TBA4A_BOVIN]	6.2×10^{6}
Transforming growth factor-beta-induced protein ig-h3 OS=Bos taurus O×=9913 GN=TGFBI PE=1 SV=2 - [BGH3_BOVIN]	6.2×10^{6}
Glutathione pero×idase 3 OS=Bos taurus O×=9913 GN=GP×3 PE=2 SV=2 - [GP×3_BOVIN]	6.1×10^{6}
Ferritin heavy chain OS=Bos taurus O×=9913 GN=FTH1 PE=2 SV=3 - [FRIH_BOVIN]	6.1×10^{6}
3-hydro×yisobutyrate dehydrogenase, mitochondrial OS=Bos taurus O×=9913 GN=HIBADH PE=2 SV=1 - [3HIDH_BOVIN]	5.7×10^{6}
NAD(P)H-hydrate epimerase OS=Bos taurus O×=9913 GN=NA×E PE=2 SV=1 - [NNRE_BOVIN]	5.4×10^{6}
Translationally-controlled tumor protein OS=Bos taurus O×=9913 GN=TPT1 PE=2 SV=1 - [TCTP_BOVIN]	5.2×10^{6}

Tryptophan--tRNA ligase, cytoplasmic OS=Bos taurus O×=9913 GN=WARS PE=1 SV=3 - [SYWC_BOVIN]	5.2×10^6
Prothymosin alpha OS=Bos taurus O×=9913 GN=PTMA PE=1 SV=2 - [PTMA_BOVIN]	5.1×10^6
Dihydropyrimidinase-related protein 2 OS=Bos taurus O×=9913 GN=DPYSL2 PE=1 SV=1 - [DPYL2_BOVIN]	4.9×10^6
Microtubule-associated protein 4 OS=Bos taurus O×=9913 GN=MAP4 PE=1 SV=1 - [MAP4_BOVIN]	4.9×10^6
Inter-alpha-trypsin inhibitor heavy chain H1 OS=Bos taurus O×=9913 GN=ITIH1 PE=1 SV=1 - [ITIH1_BOVIN]	4.8×10^6
Proteasome subunit alpha type-1 OS=Bos taurus O×=9913 GN=PSMA1 PE=1 SV=1 - [PSA1_BOVIN]	4.8×10^6
Fibulin-5 OS=Bos taurus O×=9913 GN=FBLN5 PE=2 SV=1 - [FBLN5_BOVIN]	4.6×10^6
Anne×in A11 OS=Bos taurus O×=9913 GN=AN×A11 PE=1 SV=1 - [AN×11_BOVIN]	4.5×10^6
Protein disulfide-isomerase OS=Bos taurus O×=9913 GN=P4HB PE=1 SV=1 - [PDIA1_BOVIN]	4.2×10^6
[Protein ADP-ribosylarginine] hydrolase-like protein 1 OS=Bos taurus O×=9913 GN=ADPRHL1 PE=2 SV=1 - [ARHL1_BOVIN]	3.9×10^6
Calpastatin OS=Bos taurus O×=9913 GN=CAST PE=1 SV=2 - [ICAL_BOVIN]	3.8×10^6
Mannose-6-phosphate isomerase OS=Bos taurus O×=9913 GN=MPI PE=2 SV=3 - [MPI_BOVIN]	3.8×10^6
UV e×cision repair protein RAD23 homolog B OS=Bos taurus O×=9913 GN=RAD23B PE=2 SV=1 - [RD23B_BOVIN]	3.7×10^6
SH3 domain-binding glutamic acid-rich-like protein 3 OS=Bos taurus O×=9913 GN=SH3BGRL3 PE=3 SV=1 - [SH3L3_BOVIN]	3.7×10^6
Ubiquitin-conjugating enzyme E2 L3 OS=Bos taurus O×=9913 GN=UBE2L3 PE=2 SV=1 - [UB2L3_BOVIN]	3.6×10^6
Cysteine and glycine-rich protein 1 OS=Bos taurus O×=9913 GN=CSRP1 PE=2 SV=3 - [CSRP1_BOVIN]	3.6×10^6
cAMP-dependent protein kinase type II-alpha regulatory subunit OS=Bos taurus O×=9913 GN=PRKAR2A PE=1 SV=2 - [KAP2_BOVIN]	3.6×10^6
Heterogeneous nuclear ribonucleoprotein K OS=Bos taurus O×=9913 GN=HNRNPK PE=2 SV=1 - [HNRPK_BOVIN]	3.5×10^6

Probable C->U-editing enzyme APOBEC-2 OS=Bos taurus O×=9913 GN=APOBEC2 PE=2 SV=1 - [ABEC2_BOVIN]	3.4×10^{6}
Pyrido×al phosphate homeostasis protein OS=Bos taurus O×=9913 GN=PLPBP PE=2 SV=1 - [PLPHP_BOVIN]	3.4×10^{6}
Serine/threonine-protein phosphatase 2A catalytic subunit beta isoform OS=Bos taurus O×=9913 GN=PPP2CB PE=1 SV=1 - [PP2AB_BOVIN]	3.2×10^{6}
NAD-dependent protein deacylase sirtuin-5, mitochondrial OS=Bos taurus O×=9913 GN=SIRT5 PE=2 SV=1 - [SIR5_BOVIN]	3.2×10^{6}
Eukaryotic translation initiation factor 4H OS=Bos taurus O×=9913 GN=EIF4H PE=2 SV=1 - [IF4H_BOVIN]	2.8×10^{6}
Delta-aminolevulinic acid dehydratase OS=Bos taurus O×=9913 GN=ALAD PE=2 SV=1 - [HEM2_BOVIN]	2.7×10^{6}
Heterogeneous nuclear ribonucleoproteins A2/B1 OS=Bos taurus O×=9913 GN=HNRNPA2B1 PE=2 SV=1 - [ROA2_BOVIN]	2.6×10^{6}
Antithrombin-III OS=Bos taurus O×=9913 GN=SERPINC1 PE=1 SV=2 - [ANT3_BOVIN]	2.5×10^{6}
2-o×oglutarate dehydrogenase, mitochondrial OS=Bos taurus O×=9913 GN=OGDH PE=2 SV=1 - [ODO1_BOVIN]	2.5×10^{6}
Eukaryotic translation initiation factor 3 subunit J OS=Bos taurus O×=9913 GN=EIF3J PE=2 SV=1 - [EIF3J_BOVIN]	2.0×10^{6}
Transaldolase OS=Bos taurus O×=9913 GN=TALDO1 PE=2 SV=1 - [TALDO_BOVIN]	2.0×10^{6}
CapZ-interacting protein OS=Bos taurus O×=9913 GN=RCSD1 PE=2 SV=1 - [CPZIP_BOVIN]	1.9×10^{6}
Protein disulfide-isomerase A4 OS=Bos taurus O×=9913 GN=PDIA4 PE=2 SV=1 - [PDIA4_BOVIN]	1.9×10^{6}
ATP synthase subunit gamma, mitochondrial OS=Bos taurus O×=9913 GN=ATP5F1C PE=1 SV=3 - [ATPG_BOVIN]	1.4×10^{6}
Glycerol-3-phosphate phosphatase OS=Bos taurus O×=9913 GN=PGP PE=2 SV=1 - [PGP_BOVIN]	1.4×10^{6}
Tubulin-folding cofactor B OS=Bos taurus O×=9913 GN=TBCB PE=2 SV=1 - [TBCB_BOVIN]	9.4×10^{5}